Marianne Liebi– Material Science at Large Scale Facilities

Coherent Diffraction Imaging

EPFL Master Course 2025 MSE435

Course program

Dates	Content	Lecturer
08.09.25	Introduction, sources, beamlines, detectors	Steven Van Petegem
15.09.25	Excursion to PSI	Marianne Liebi
22.09.25	Holiday	
29.09.25	Interaction with matter	Steven Van Petegem
06.10.25	Fluorescence	Marianne Liebi
13.10.25	X-ray absorption spectroscopy	Marianne Liebi
20.10.25	Break	
27.10.25	Diffraction I	Steven Van Petegem
03.11.25	Small angle scattering	Marianne Liebi
10.11.25	Diffraction II	Steven Van Petegem
17.11.25	Phase contrast / Tomography	Steven Van Petegem
24.11.25	Coherent imaging	Marianne Liebi
01.12.25	Neutron imaging	Steven Van Petegem
08.12.25	PEEM / Magnetic scattering	Steven Van Petegem
15.12.25	Case study presentations	Steven Van Petegem / Marianne Liebi

Far-field Fraunhofer Regim

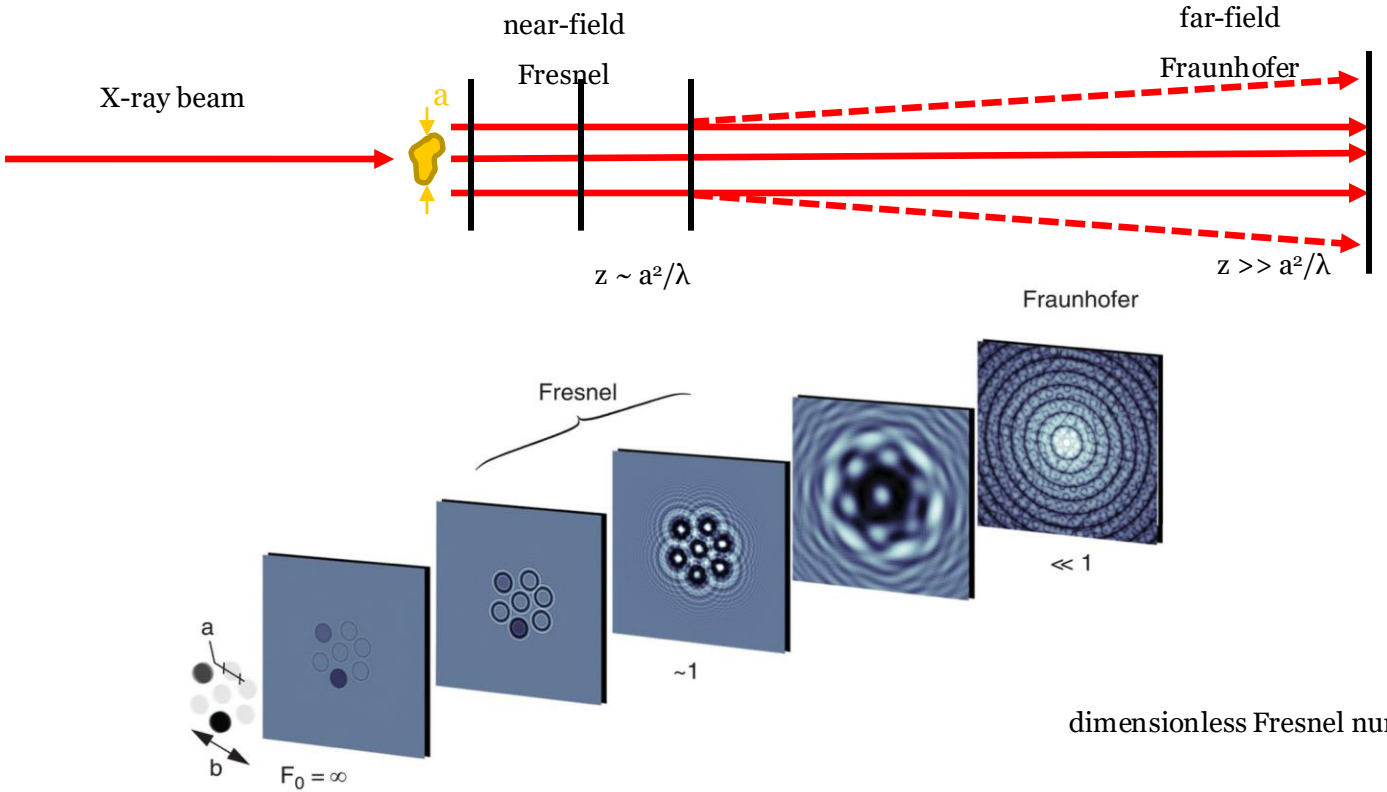

dimensionless Fresnel number $F_o=a^2/z\lambda$

Willmott, P., John Wiley & Sons, Ltd: 2019 (2nd Edition).

X-ray imaging: full-field

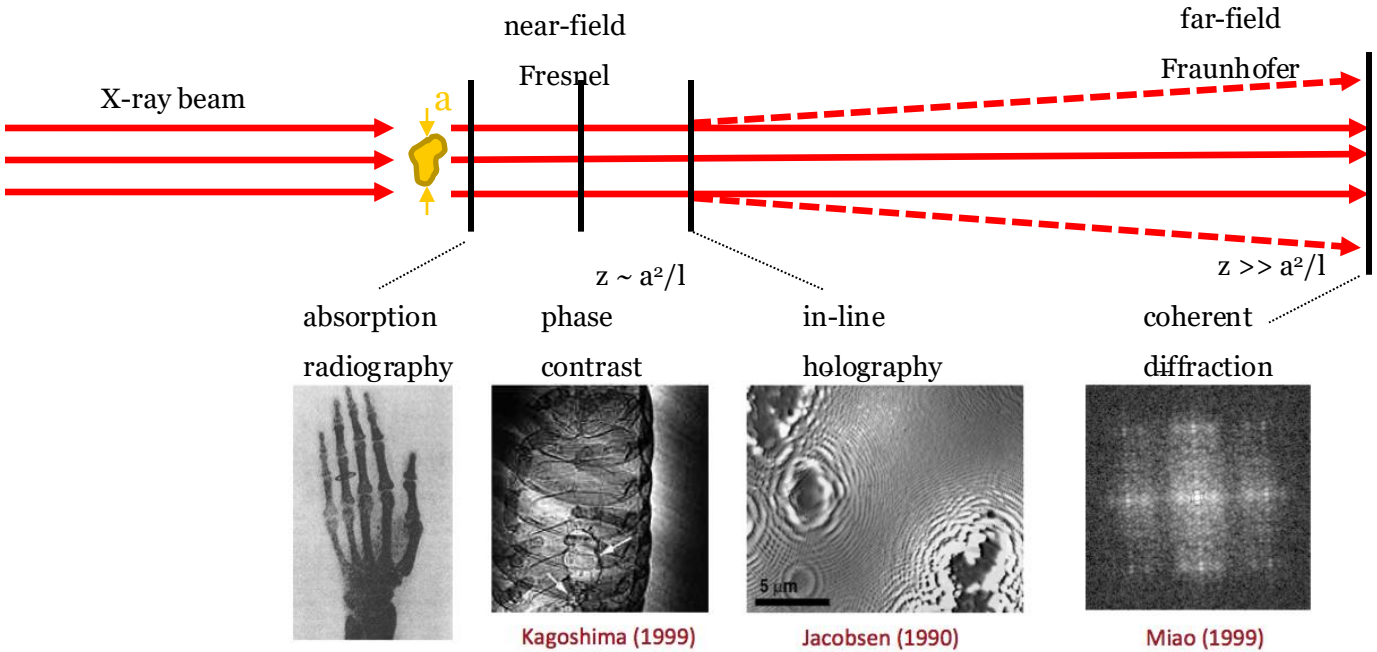

Interaction of X-rays with matter

interaction with electrons

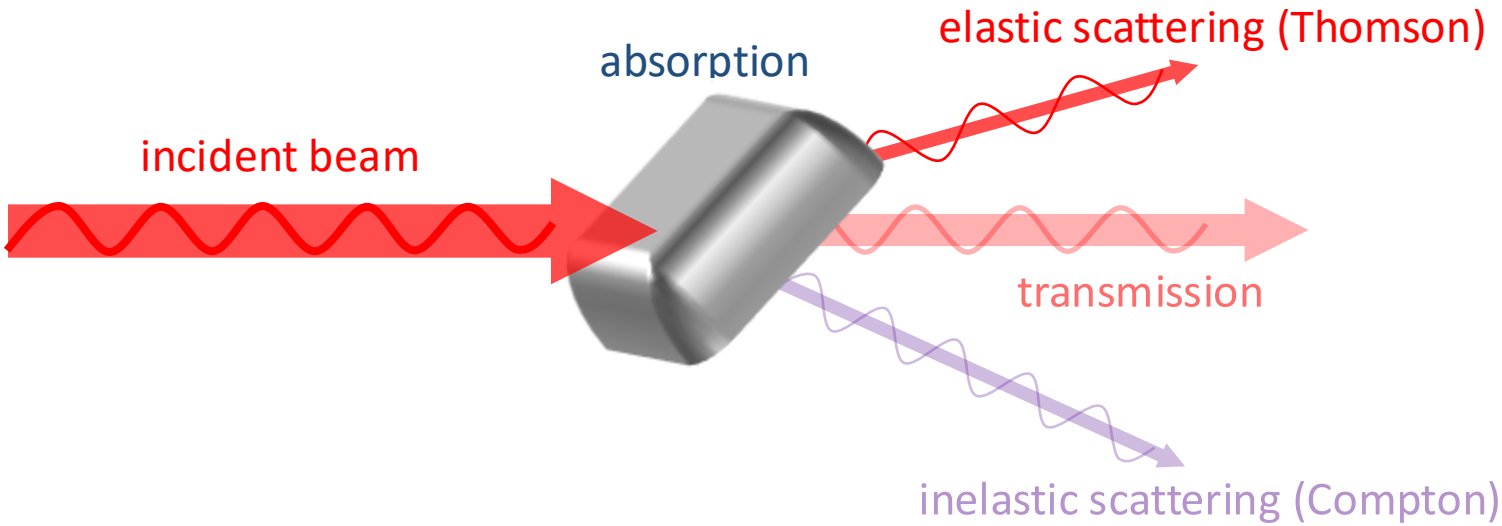

Longitudinal coherence

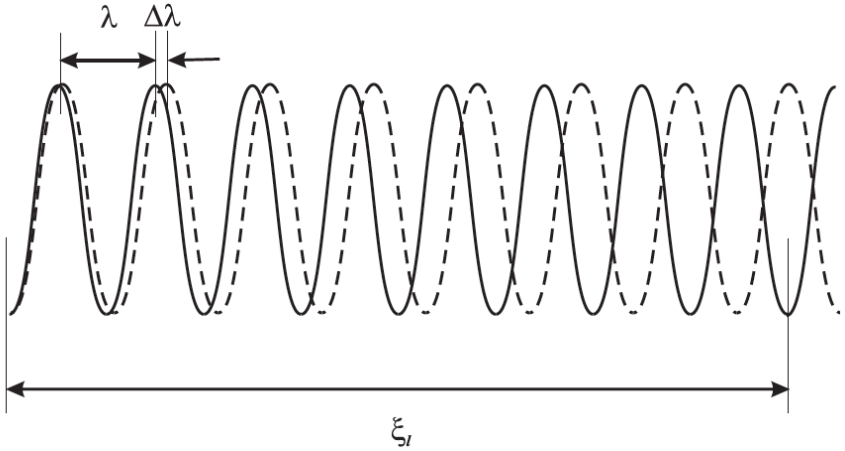

Longitudinal coherence length: $\xi_l \simeq \frac{1}{2}\frac{\lambda^2}{\Delta\lambda}$

"Propagation of two waves with wavelengths λ and l + Δλ. The longitudinal coherence length is defined as the distance over which the phase difference between the two waves is π."

J. F. Van der Veen & F. Pfeiffer J. Phys.: Condens. Matter **16**, 5003 (2004)

Longitudinal coherence

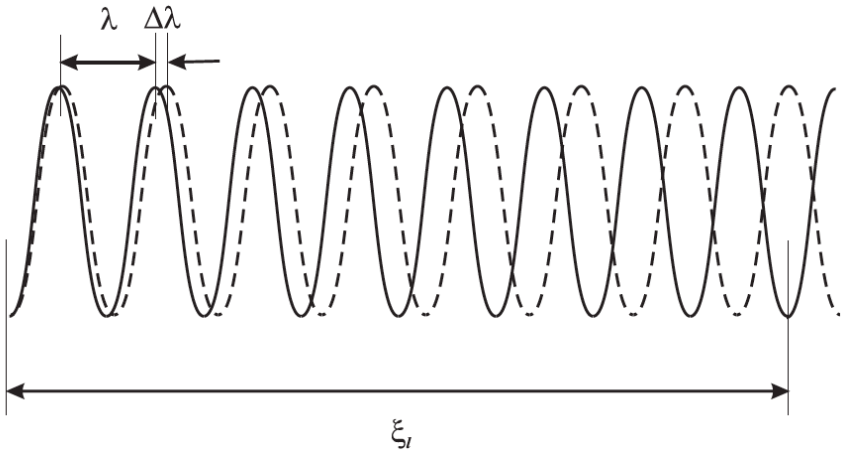

Longitudinal coherence length: $\xi_l \simeq \frac{1}{2}\frac{\lambda^2}{\Delta\lambda}$

Si (111) monochromator: $Dl/l = 1.3\times10^{-4}$

l = 2 Å ➔ $\zeta_l \approx$ 800 nm

J. F. Van der Veen & F. Pfeiffer J. Phys.: Condens. Matter **16**, 5003 (2004)

Implications of longitudinal coherence

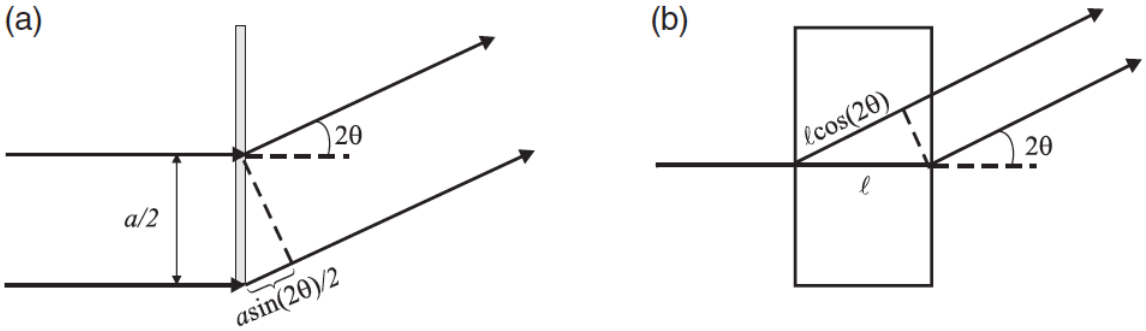

A condition for coherence is that the path length difference between points scattered from different points at the sample is smaller than the longitudinal coherence length x_l

$$\frac{\Delta\lambda}{\lambda} < \frac{s}{a}$$

In order to resolve an object of size a = 5 µm to within s = 10 nm, one has to keep the bandwith below 2×10^{-3} → crystal monochromator

J. F. Van der Veen & F. Pfeiffer J. Phys.: Condens. Matter **16**, 5003 (2004)

Transversal coherence

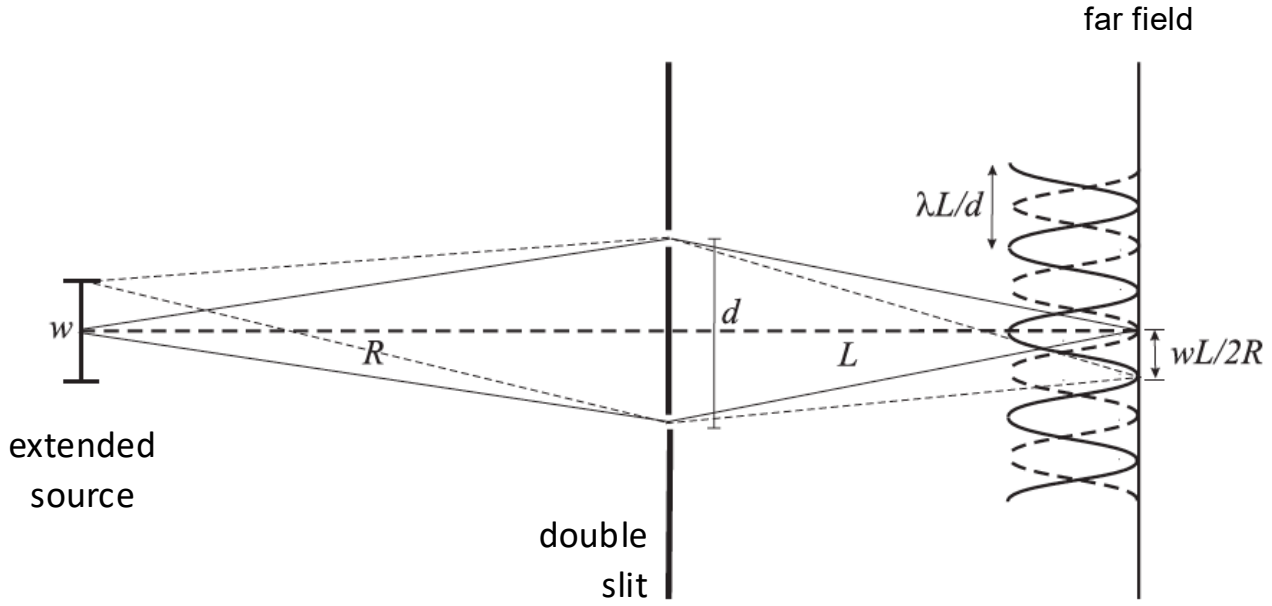

Transversal coherence length: $\xi_t = \frac{\lambda R}{w}$

Maximum distance between two slits such that they produce constructive interference when illuminated by an extended source size

J. F. Van der Veen & F. Pfeiffer J. Phys.: Condens. Matter **16**, 5003 (2004)

Transversal coherence

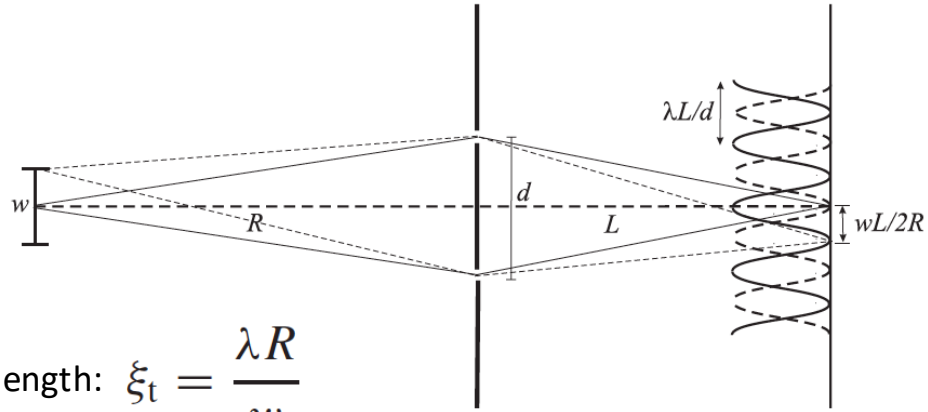

Transversal coherence length: $\xi_t = \frac{\lambda R}{w}$

Laboratory: $x_h < 1$ µm

Numbers for a typical 3rd generation source

λ = 2 Å

R = 34 m

w_v = 20 µm ➔ x_v = 340 µm

w_h = 200 µm ➔ x_h = 34 µm

SLS 2.0 (cSAXS)

λ = 2 Å

R = 33 m

w_v = 12 µm ➔ x_v = 550 µm

w_h = 47 µm ➔ x_h = 140 µm

J. F. Van der Veen & F. Pfeiffer J. Phys.: Condens. Matter **16**, 5003 (2004)

SLS upgrade to SLS2.0

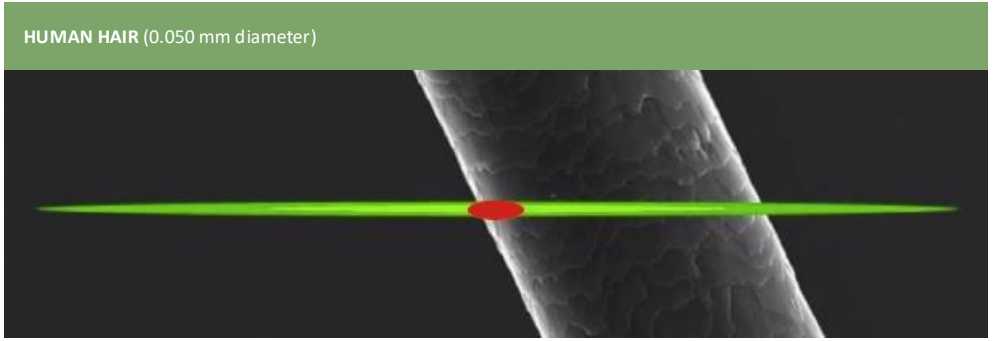

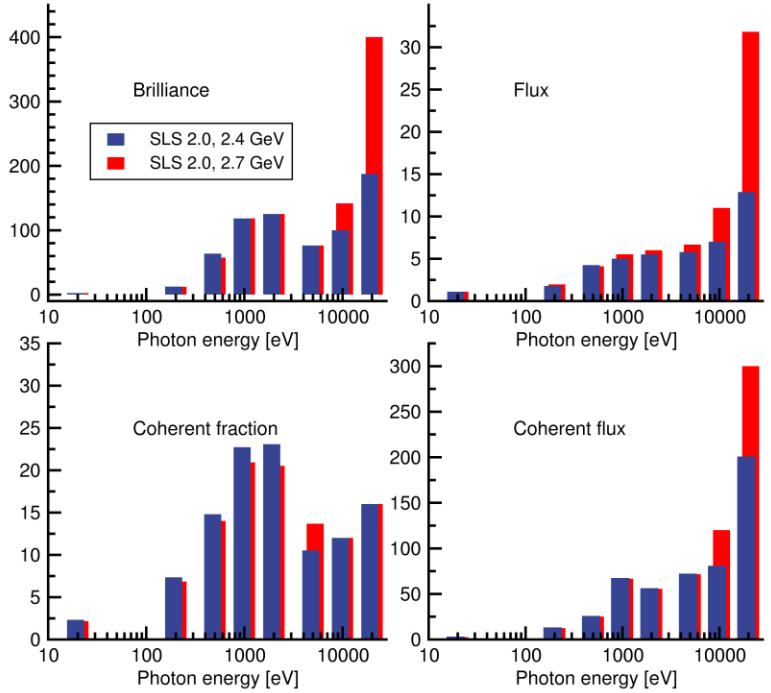

Factor improvements SLS 2.0/SLS
for most important parameters

Coherence

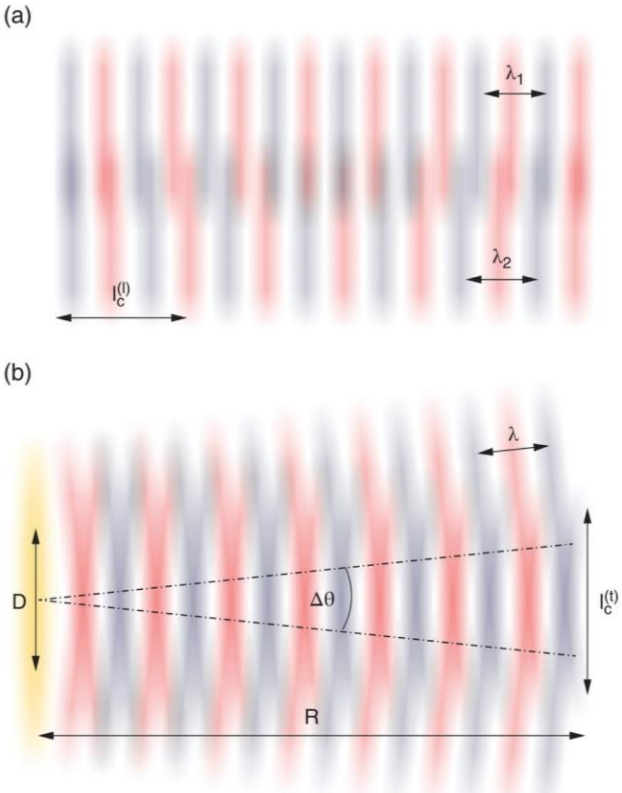

longitudinal (temporal) coherence length
determined by monochromacy of the source

transverse (spatial) coherence length
depends on the beam divergence and source size

Willmott, P. (2019). Scattering Techniques. An Introduction to Synchrotron Radiation, John Wiley & Sons, Ltd: 133-221.

small-angle X-ray scattering

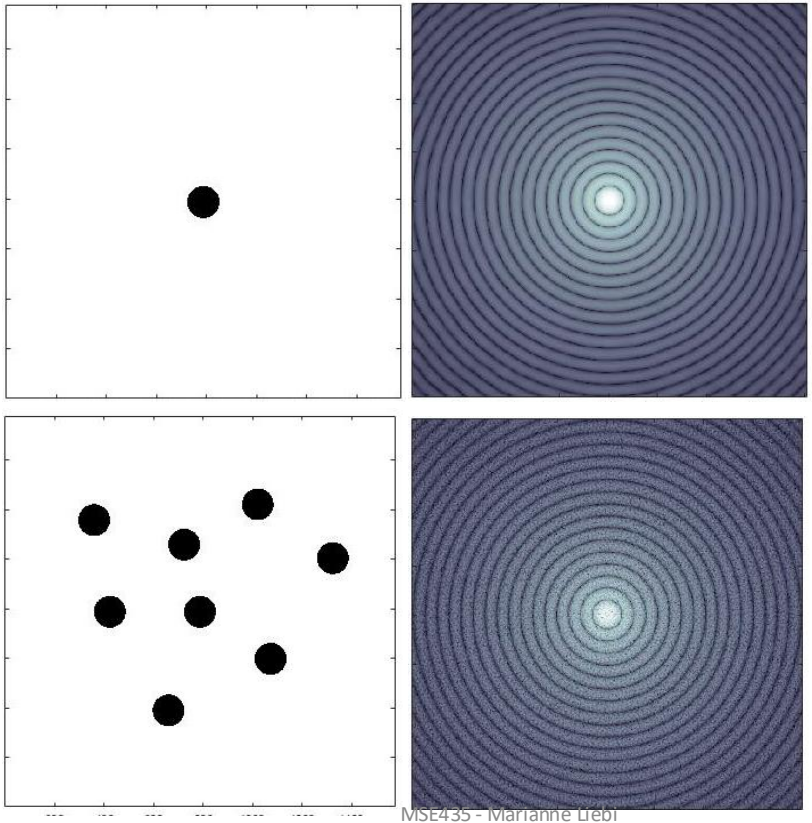

scattering pattern shows
average over particle ensemble

Scattering with coherent illumination

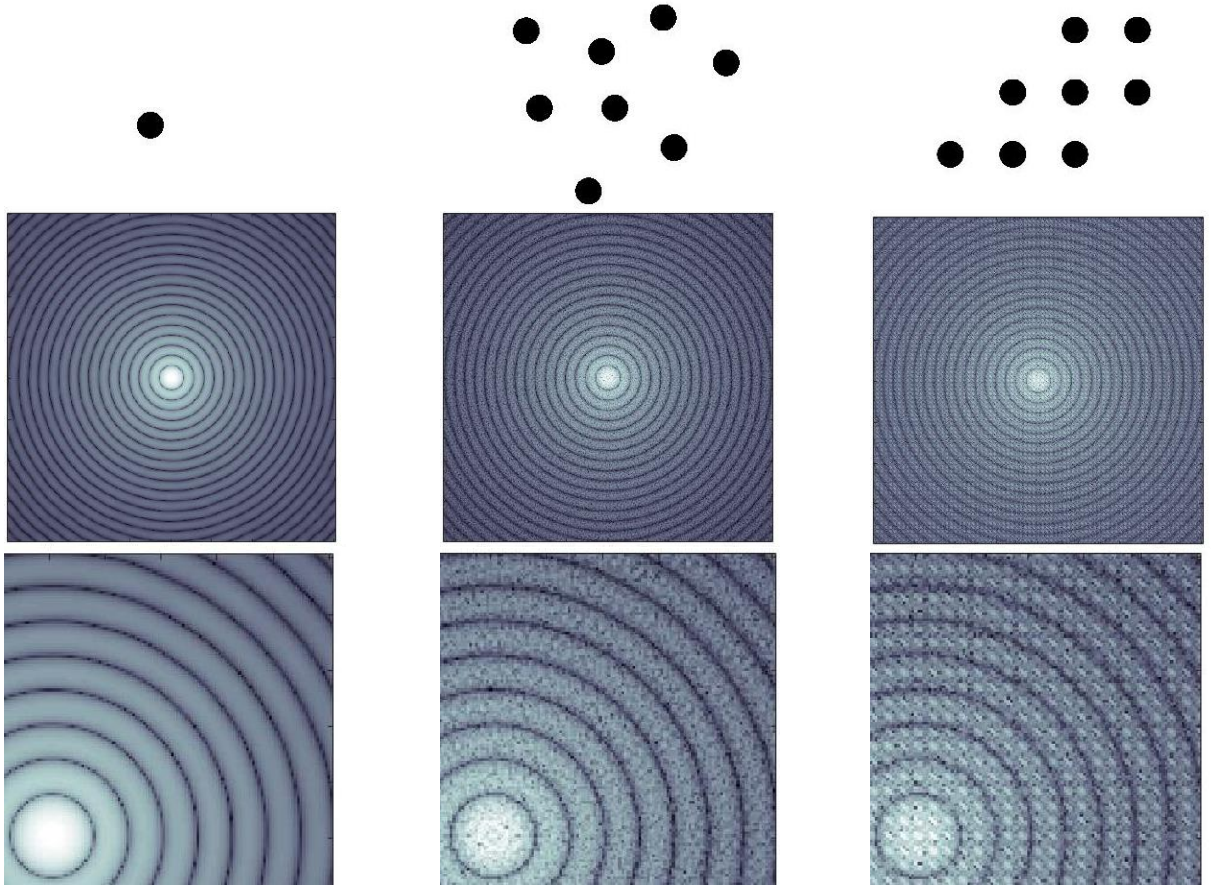

Coherent scattering

X-ray scattering from a disordered medium in the far field (Fraunhofer)

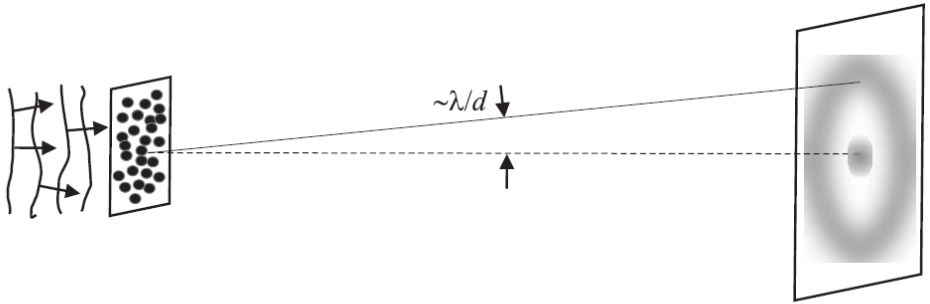

average over patterns from slightly different wavefronts

→ average over particle ensemble

with full coherent illumination: speckle pattern

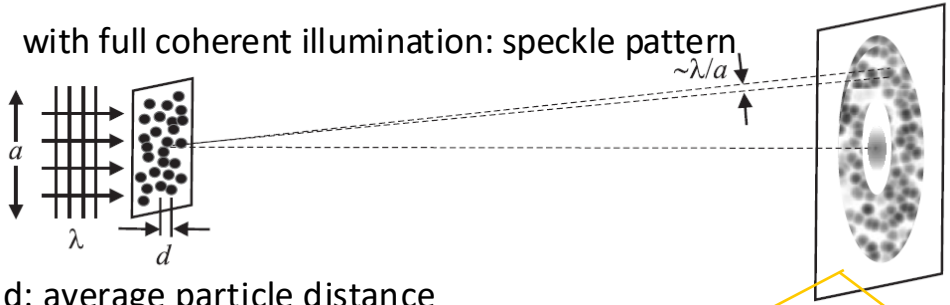

one particular realization of the system

→ no averaging over particle distance

d: average particle distance

a: size of illuminated area

dynamics: XPCS/DLS imaging

J. F. Van der Veen & F. Pfeiffer J. Phys.: Condens. Matter **16**, 5003 (2004)

Coherent diffraction imaging (CDI)

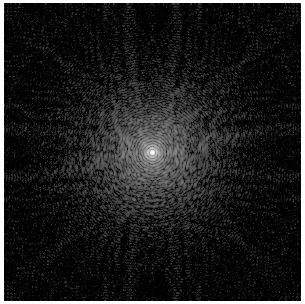

Fourier constraint

image is consistent with measured intensity

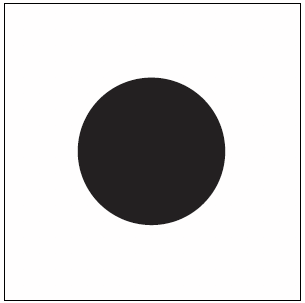

support constraint

the object is inside a finite support

Coherent diffraction imaging (CDI)

Iterative phase retrieval algorithm

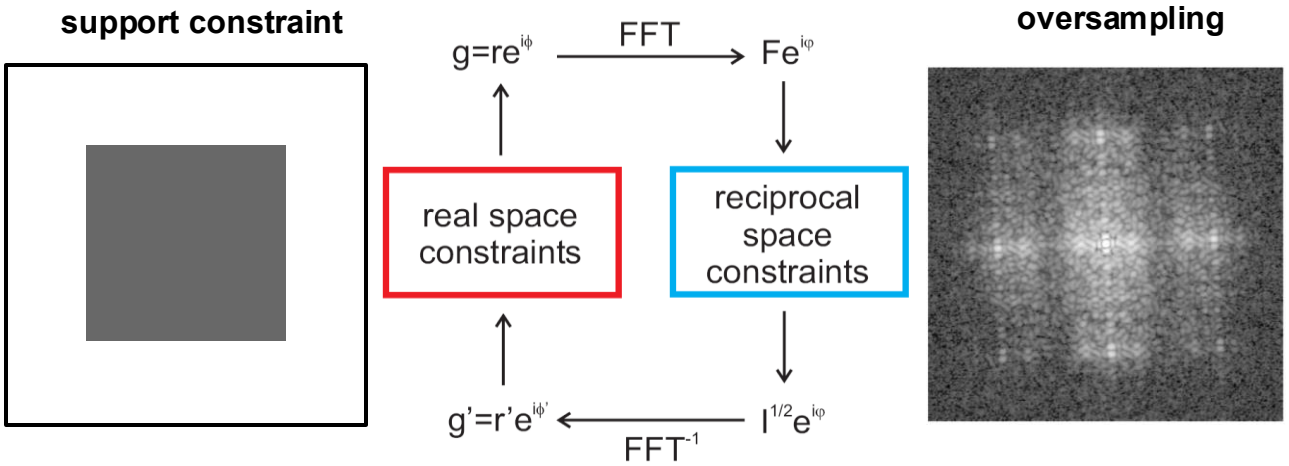

J.R. Fienup Appl. Opt. **21** (1982) 2758

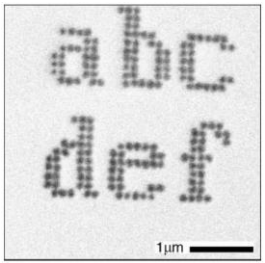

Sample consisting of
100 nm Au nanodots

J. Miao et al., Nature **400** (1999) 342

Coherent diffraction imaging (CDI)

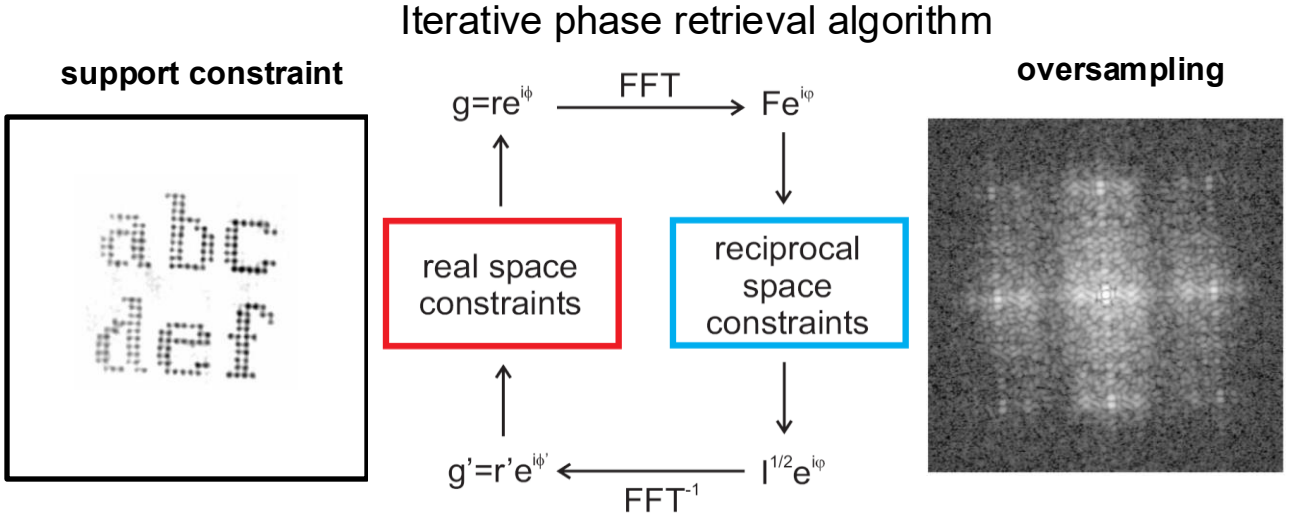

J.R. Fienup Appl. Opt. **21** (1982) 2758

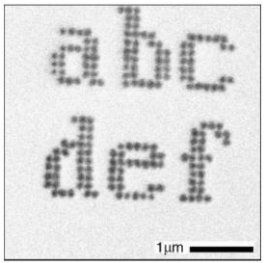

Sample consisting of
100 nm Au nanodots

- Resolution not limited by optics

J. Miao et al., Nature **400** (1999) 342

SAXS analysis: iterative approach

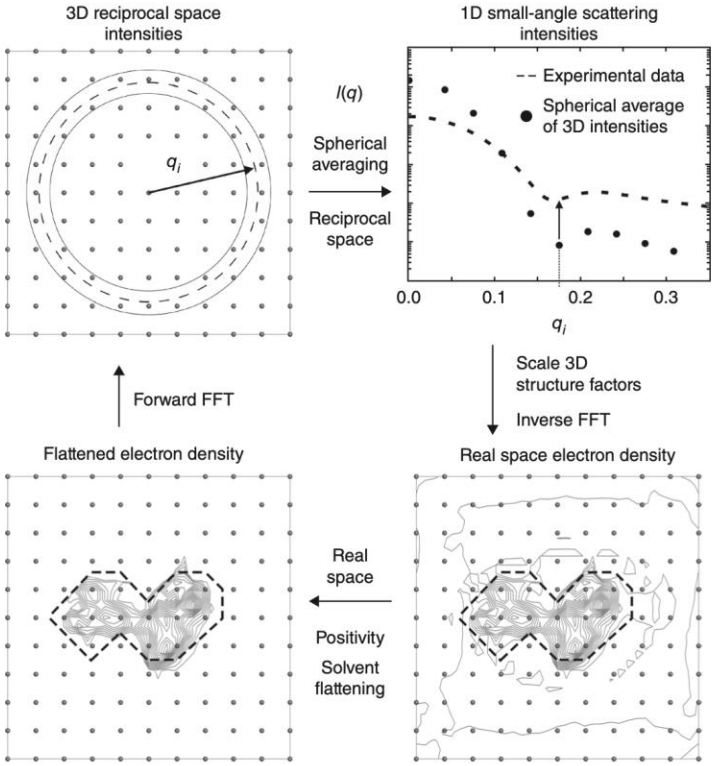

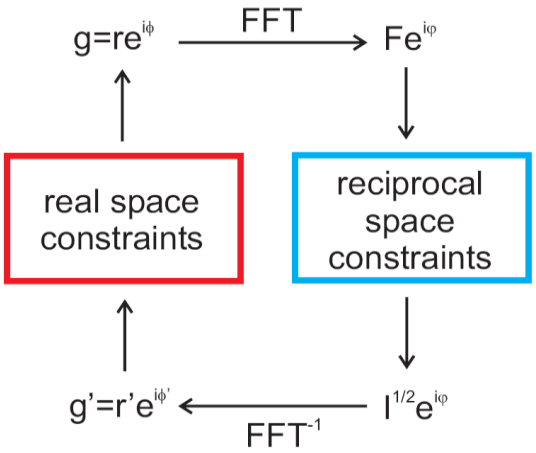

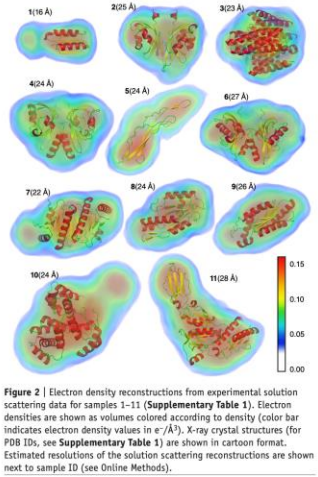

Figure 2 | Electron density reconstructions from experimental solution scattering data for samples 1–11 (**Supplementary Table 1**). Electron densities are shown as volumes colored according to density (color bar indicates electron density values in $e^-/Å^3$). X-ray crystal structures (for PDB IDs, see **Supplementary Table 1**) are shown in cartoon format. Estimated resolutions of the solution scattering reconstructions are shown next to sample ID (see Online Methods).

→ SAXS only **average** nanostructure of sample illuminated,

→ CDI image of the nanostructure illuminated

Grant, T. D., *Nature Methods* **2018,** *15*, 191.

3D coherent diffraction imaging

School of J. Miao

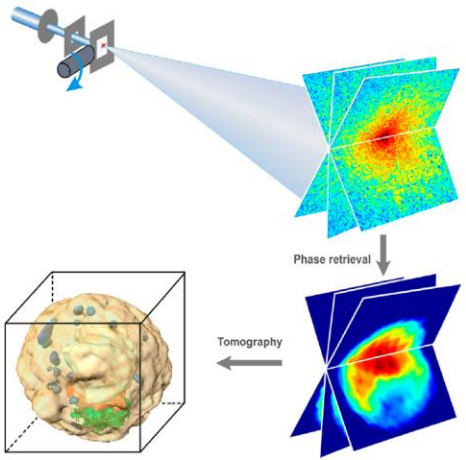

H. Jiang *et al.*,
PNAS **107** (2010) 11234

- 2D phase retrieval on each 2D coherent diffraction pattern recorded at different angles
- Conventional tomography

School of H. N. Chapman

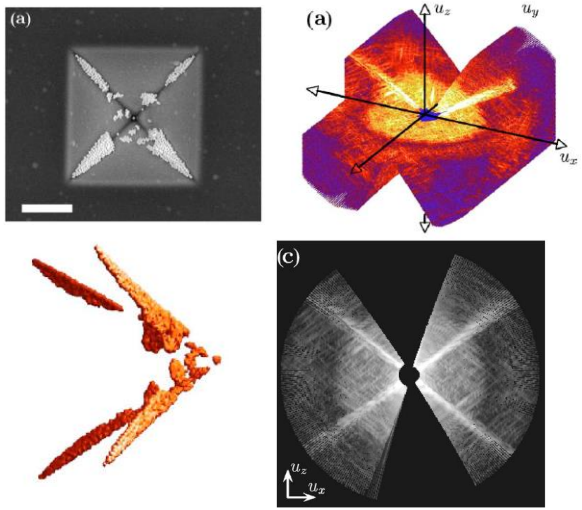

H. N. Chapman *et al.*,
J. Opt. Soc. Am. A **23** (2006) 1179

- 3D reciprocal space construction from 2D coherent diffraction patterns recorded at different angles
- 3D phase retrieval

X-ray free electron lasers (X-FELs)

Diffract-before-destroy approach

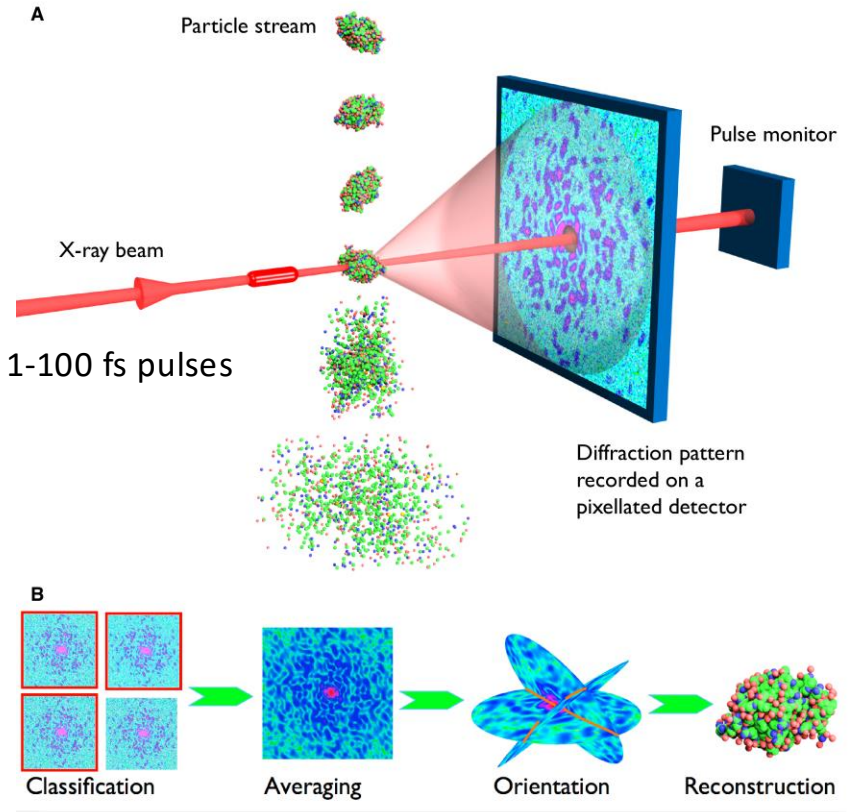

https://cid.cfel.de/research/single_particle_imaging/
Henry Chapman, CFEL. Science, 2007, 316, 1444-48.

Coherent diffraction imaging: examples

Ceramic nanofoam

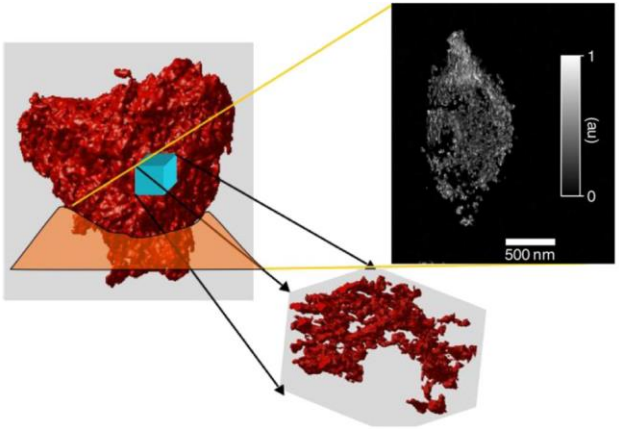

A. Barty et al., Phys. Rev. Lett. **107** (2008) 055501

Yeast spore cell

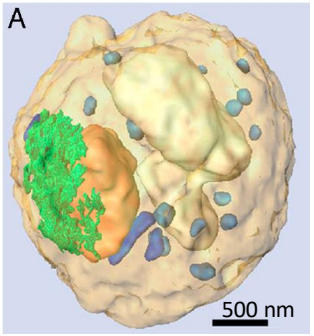

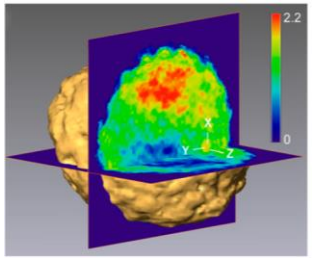

H. Jiang et al.,
PNAS **107** (2010) 11234

CDI in free electron lasers

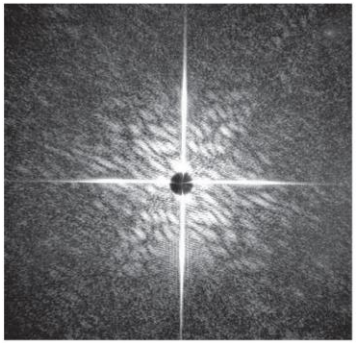

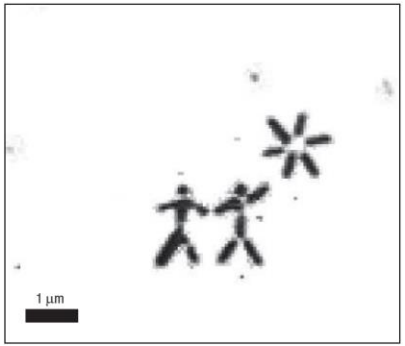

Test sample
@ FLASH, λ = 32 nm

H. N. Chapman *et al.*,
Nat. Phys. **2** (2006) 839

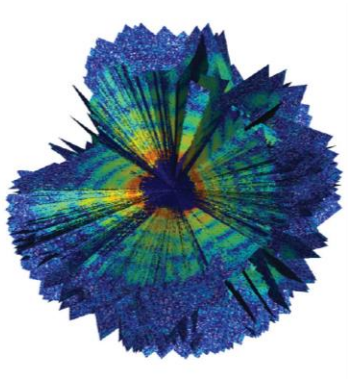

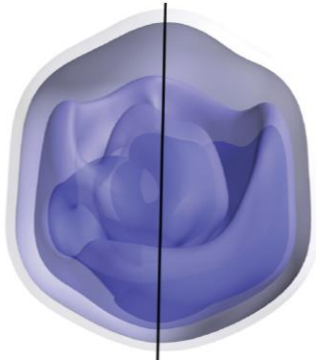

~ 450 nm

Giant mimivirus particle
@ LCLS, free electron laser

T. Ekeberg *et al.*, Phys. Rev. Lett.
114 (2015) 098102

CDI: Twin-image problem

True image

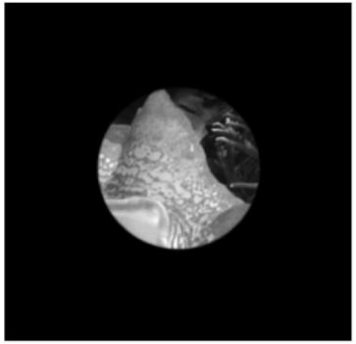

Fourier transform magnitude

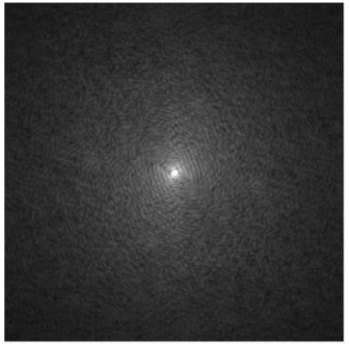

Twin image

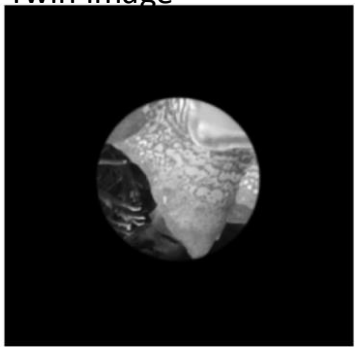

Twin image stagnation

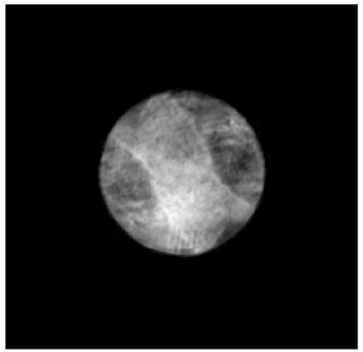

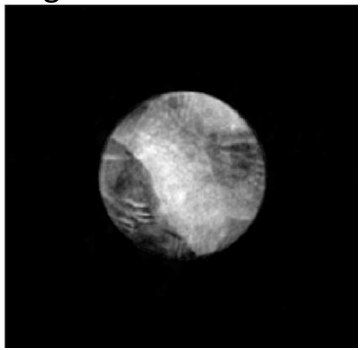

M. Guizar-Sicairos and J. R. Fienup, J. Opt. Soc. Am A **29**, 2367 (2012)

CDI

- X-ray microscopy with high resolution not limited by X-ray optics
- In Bragg geometry, it is sensitive to atomic displacements
- The convergence of the phase retrieval algorithms requires:
  - Isolated sample in 3D
  - Sample size limited to a few microns
- Practical consequences (mostly in forward direction)
  - Not robust to realistic sample preparation in many cases
  - Convergence issues
  - Typically sample lying on a membrane: missing wedge in 3D reciprocal space
  - Beamstop is often required: missing low frequencies
- CDI is done at FELs, Bragg geometry beamlines with micro- or nano-focus (Argonne, ESRF, Petra III, MAX-IV) and a few beamlines in forward direction (ESRF). Permanent setups exist for both soft and hard X-rays.

Ptychography

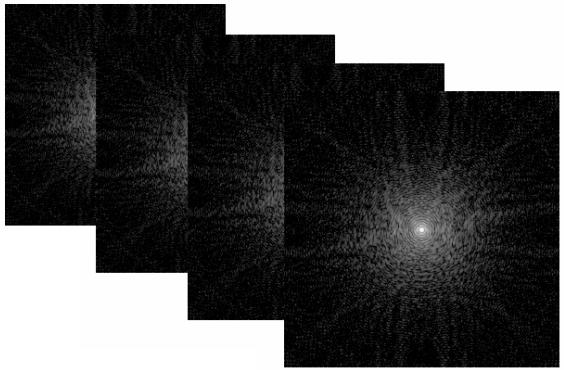

Fourier constraint

image is consistent with measured intensities

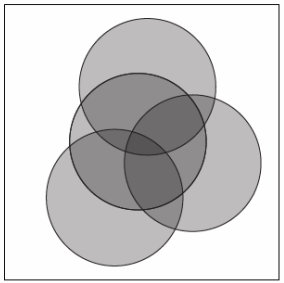

overlap constraint

overlapping regions agree and incident wave field is unique

Ptychography

oversampling by coherent diffraction patterns from overlapping regions of the specimen

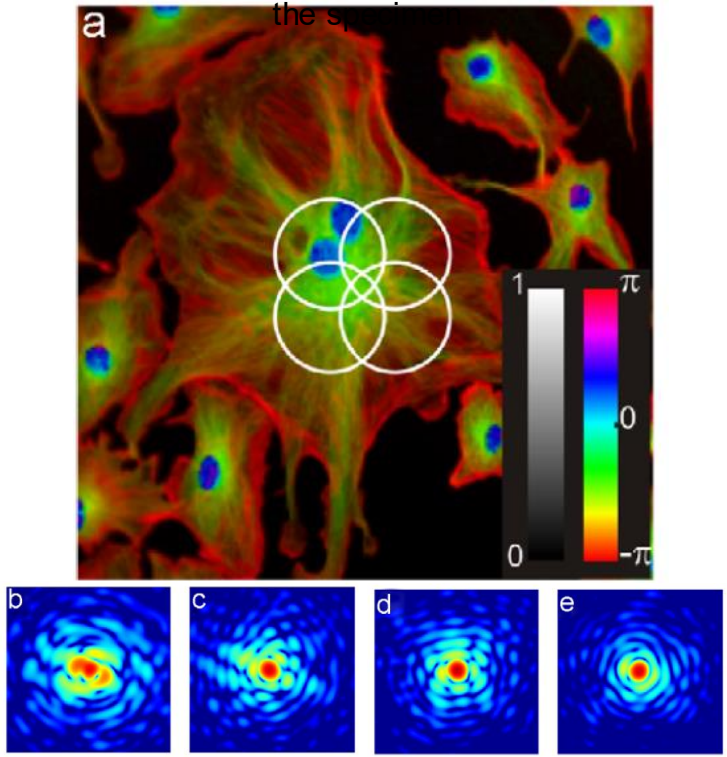

Phase retrieval algorithms to reconstruct complex-valued transmissivity

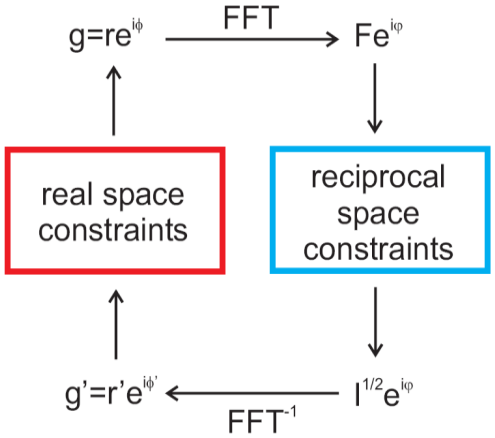

H. M. L. Faulkner & J. M. Rodenburg,

Phys. Rev. Lett. **93** (2004) 023903

Ptychography: overlap constraint

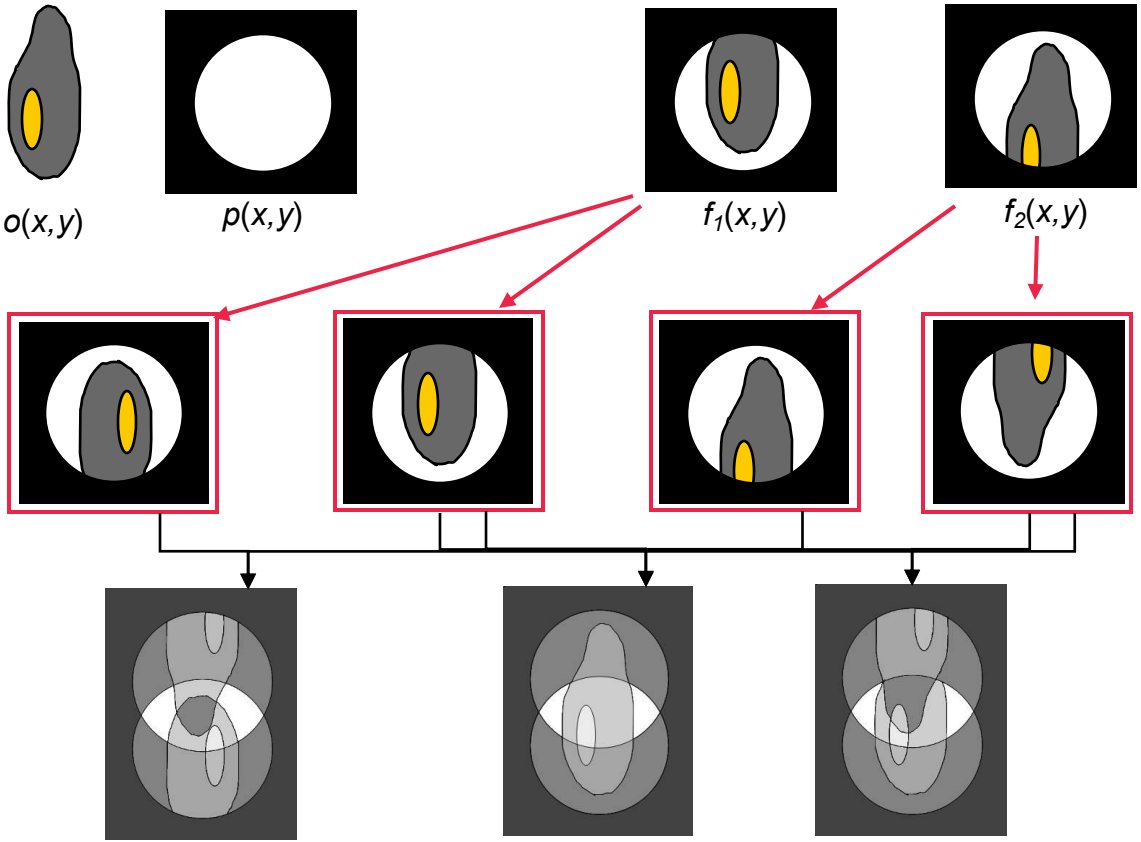

Overlap in ptychography is a crucial constraint for phase retrieval

Ptychographic nanotomography

Intel chip, 22 nm technology

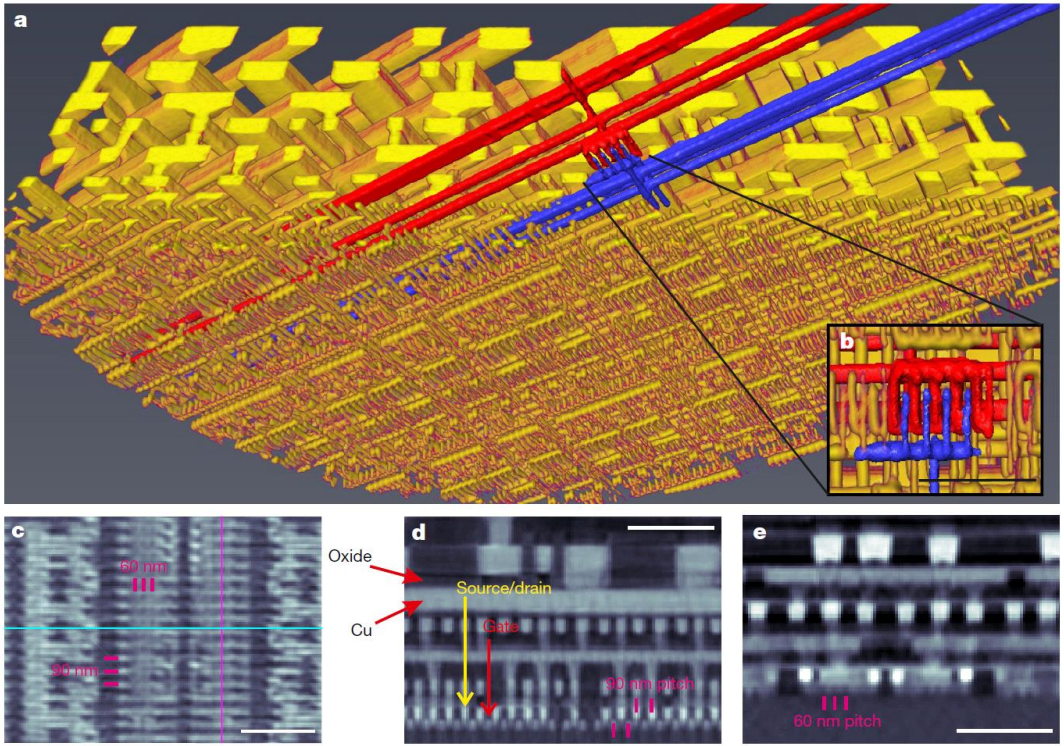

Resolution: new record: 4nm resolution

14.6 nm

Scale bars:

500 nm

M. Holler *et al.*, Nature **543** (2017) 402

Ptychographic Nanotomography

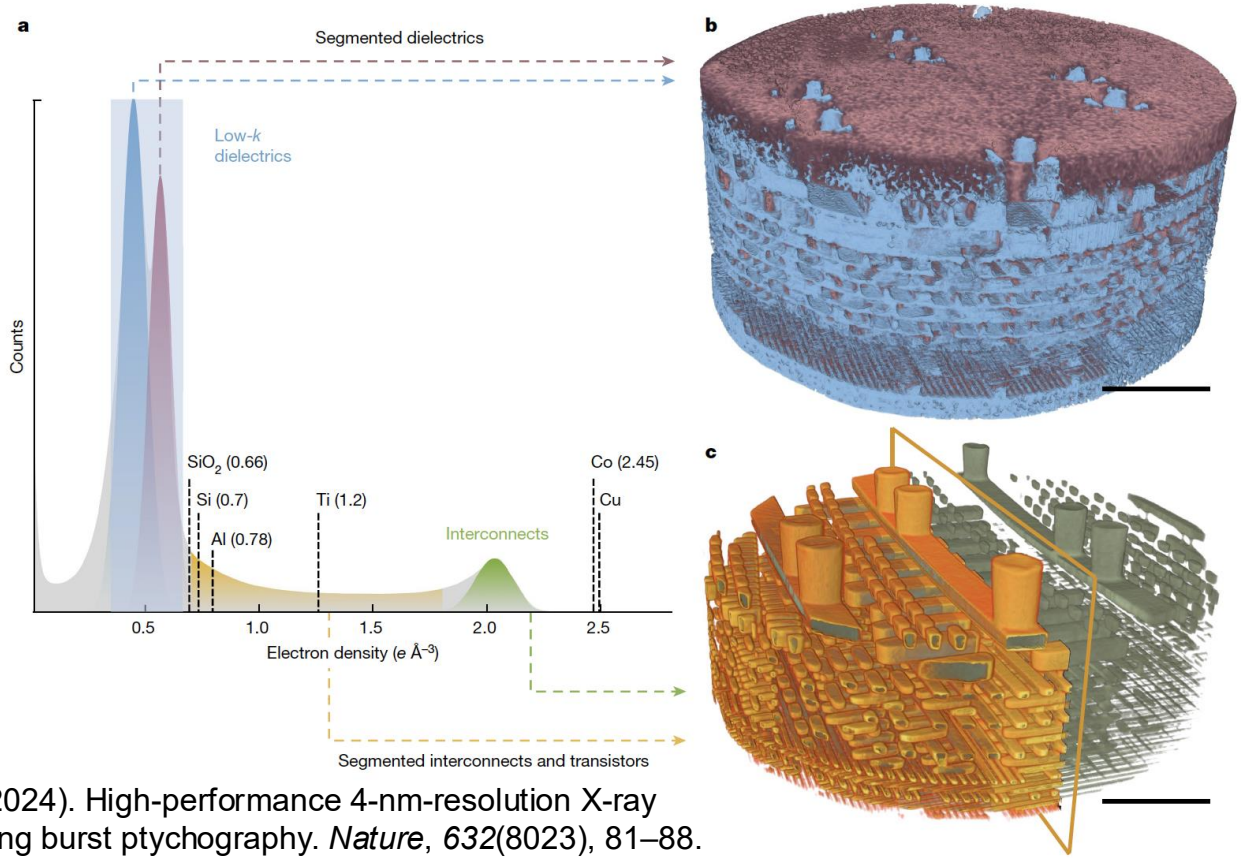

Aidukas, T., et al. (2024). High-performance 4-nm-resolution X-ray tomography using burst ptychography. *Nature*, *632*(8023), 81–88.

Ptychography with probe retrieval

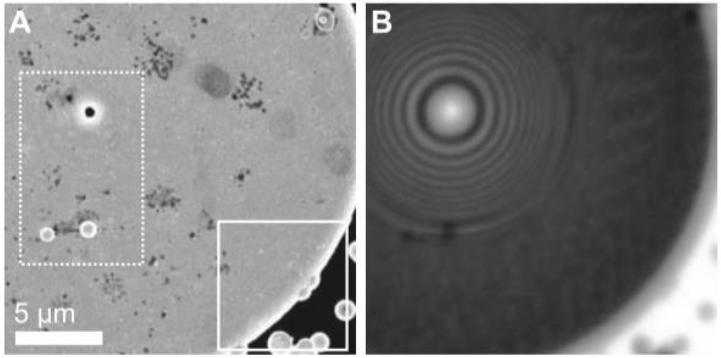

electron microscopy

gold layer on top

STXM – transmission

300 nm probe size

$$\psi_j(\mathbf{r}) = P(\mathbf{r} - \mathbf{r}_j)O(\mathbf{r})$$

Enough information to retrieve complex-valued illumination simultaneously

P. Thibault *et al.*, Science **321** (2008) 379

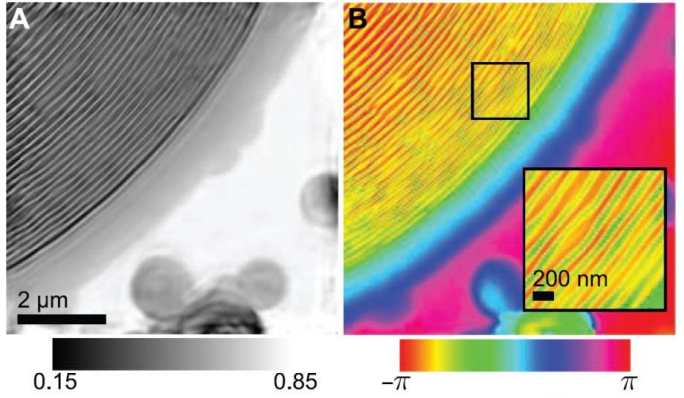

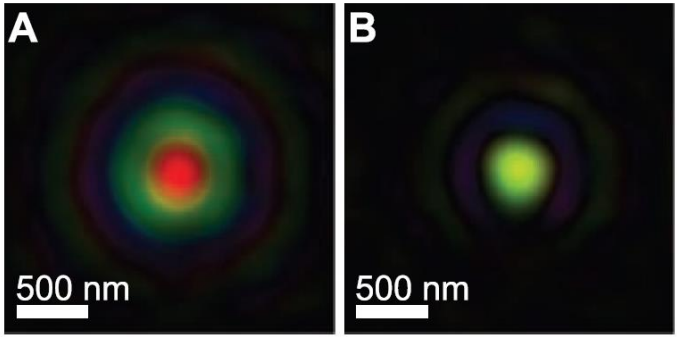

reconstructed

at sample position

back-projected

to focal plane

X-ray optics characterization with ptychography

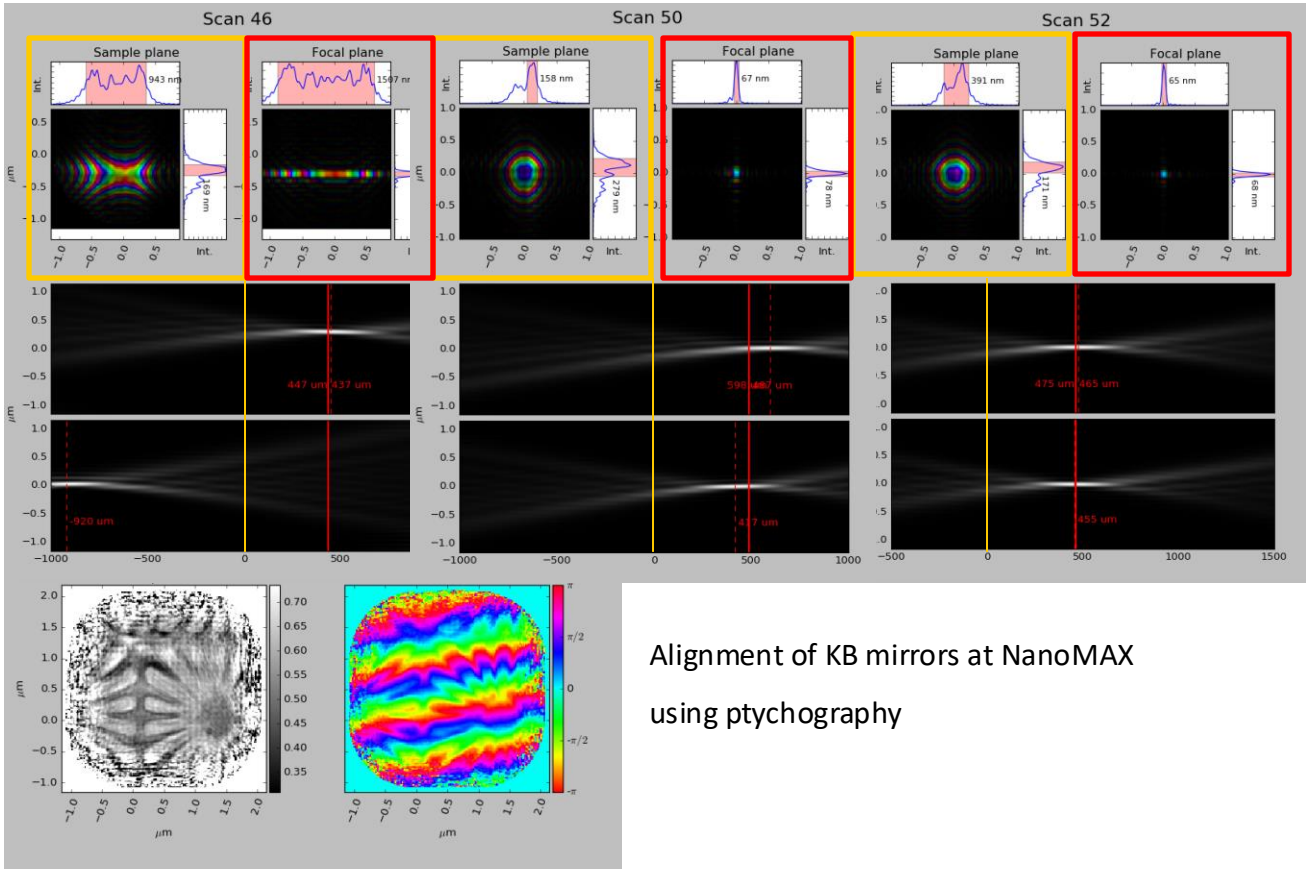

Alignment of KB mirrors at NanoMAX

using ptychography

Imaging throughput – The Eiger self portrait

Sample 5 mm downstream of focus

Beam at sample ~ 10 microns

Scanning average step 3.5 microns

Eiger as sample and detector

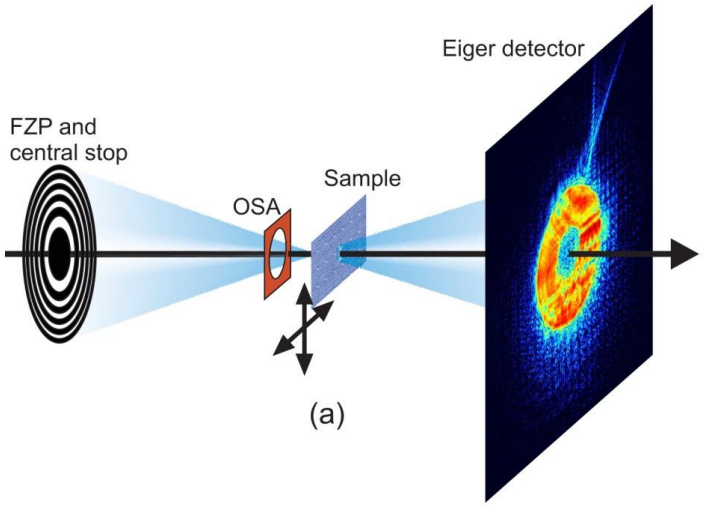

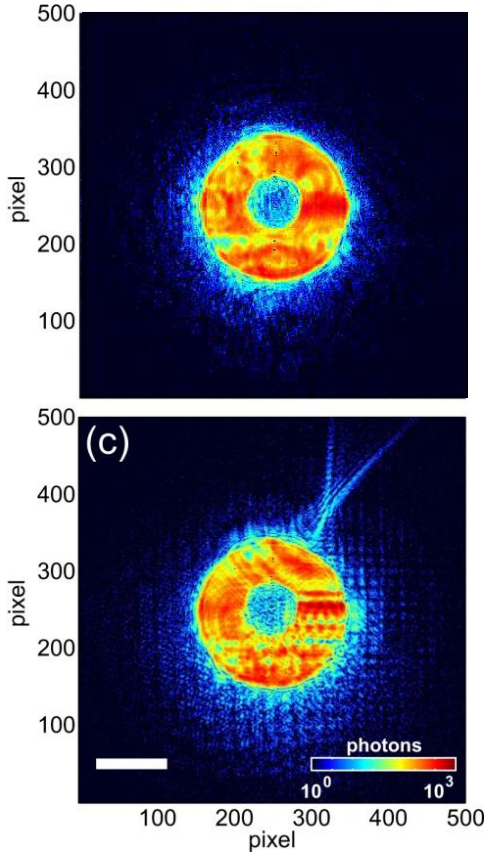

M. Guizar-Sicairos *et al.*, Opt. Express **22**, 14859 (2014)

Imaging throughput – The Eiger self portrait

98.4 Mpixel (13,028 x 7,556)
Resolution 41 nm, 38.4 nm pixel
> **25,000** resolution elements / second
40 microsecond per resolution element

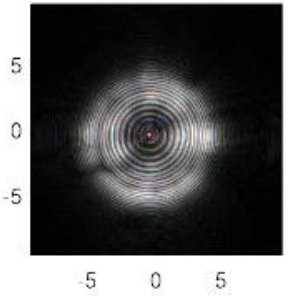

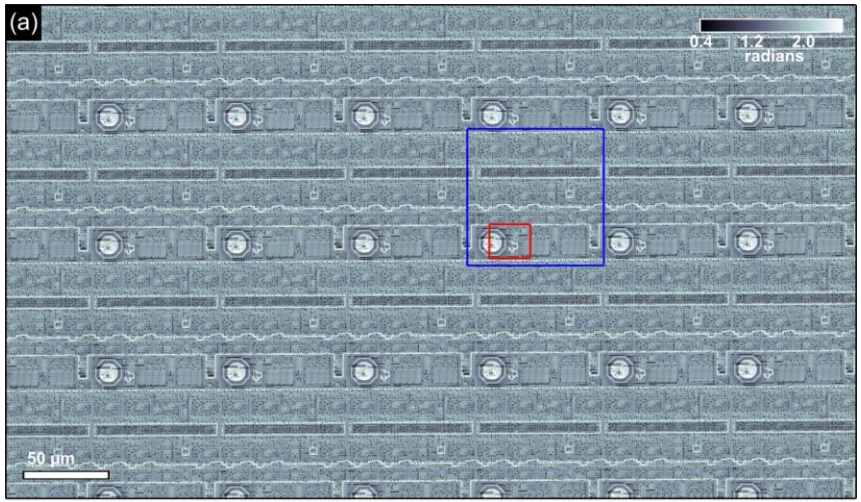

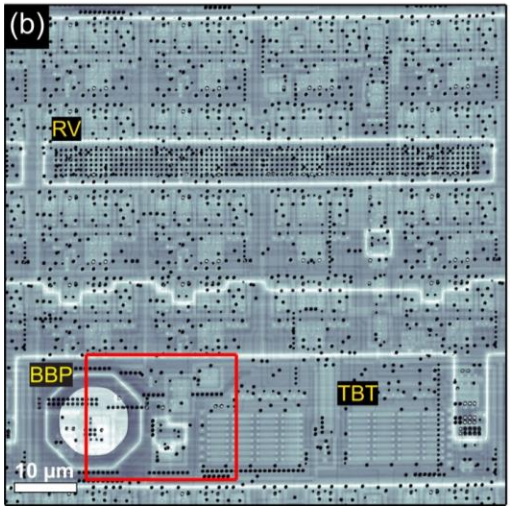

M. Guizar-Sicairos *et al.*, Opt. Express **22**, 14859 (2014)

Imaging throughput – The Eiger self portrait

98.4 Mpixel (13,028 x 7,556)
Resolution 41 nm, 38.4 nm pixel
> **25,000** resolution elements / second
40 microsecond per resolution element

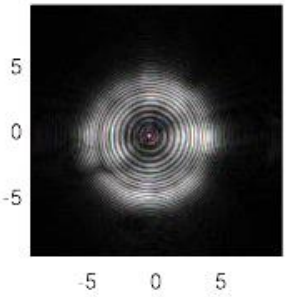

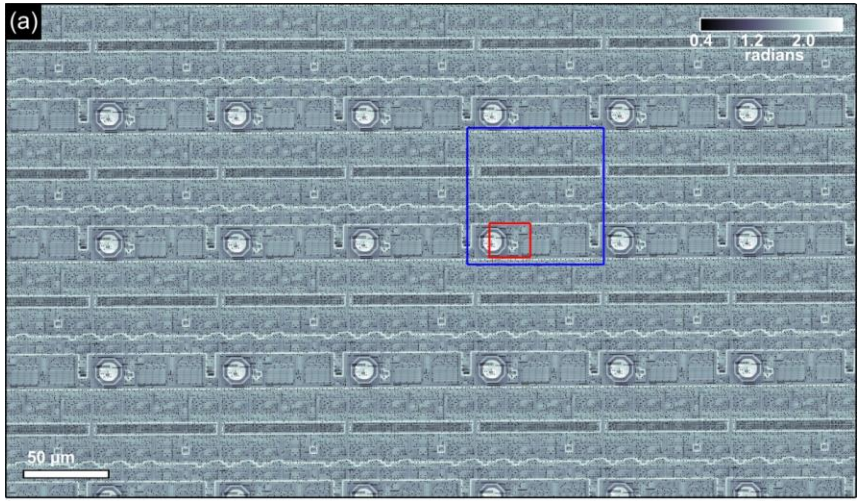

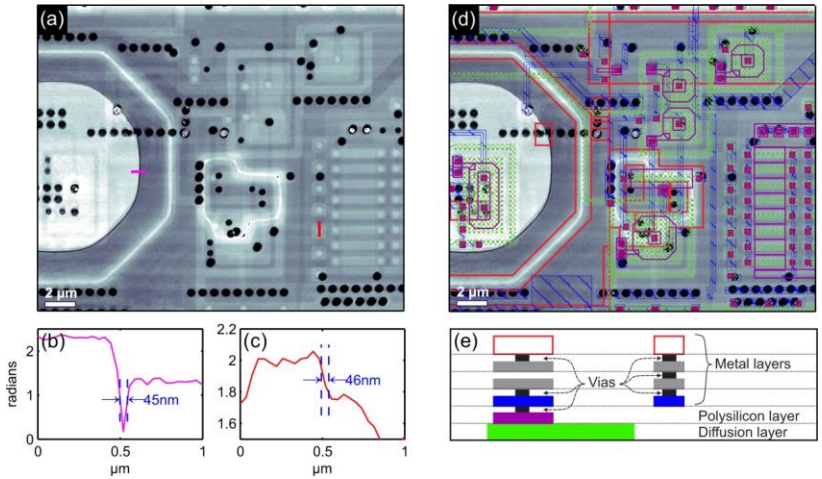

M. Guizar-Sicairos *et al.*, Opt. Express **22**, 14859 (2014)

Ptychography

- X-ray ptychography is a robust, top-quality imaging technique:
  - very high phase sensitivity
  - quantitative phase and absorption contrast
  - very high spatial resolution
- allows for extended samples (compared to CDI)
- The illumination is separated from the complex-valued transmissivity of the sample and it does not need to be a plane wave
- Requires a stable illumination and position accuracy between illumination and sample equal or better than the aimed resolution
- Practical consequences: sophisticated instrumentation, especially for 3D
- Ptychography is performed nowadays in many 3rd generation synchrotron sources worldwide and its performance is expected to be much better in 4th generation sources..

Ptychography: accurate position control

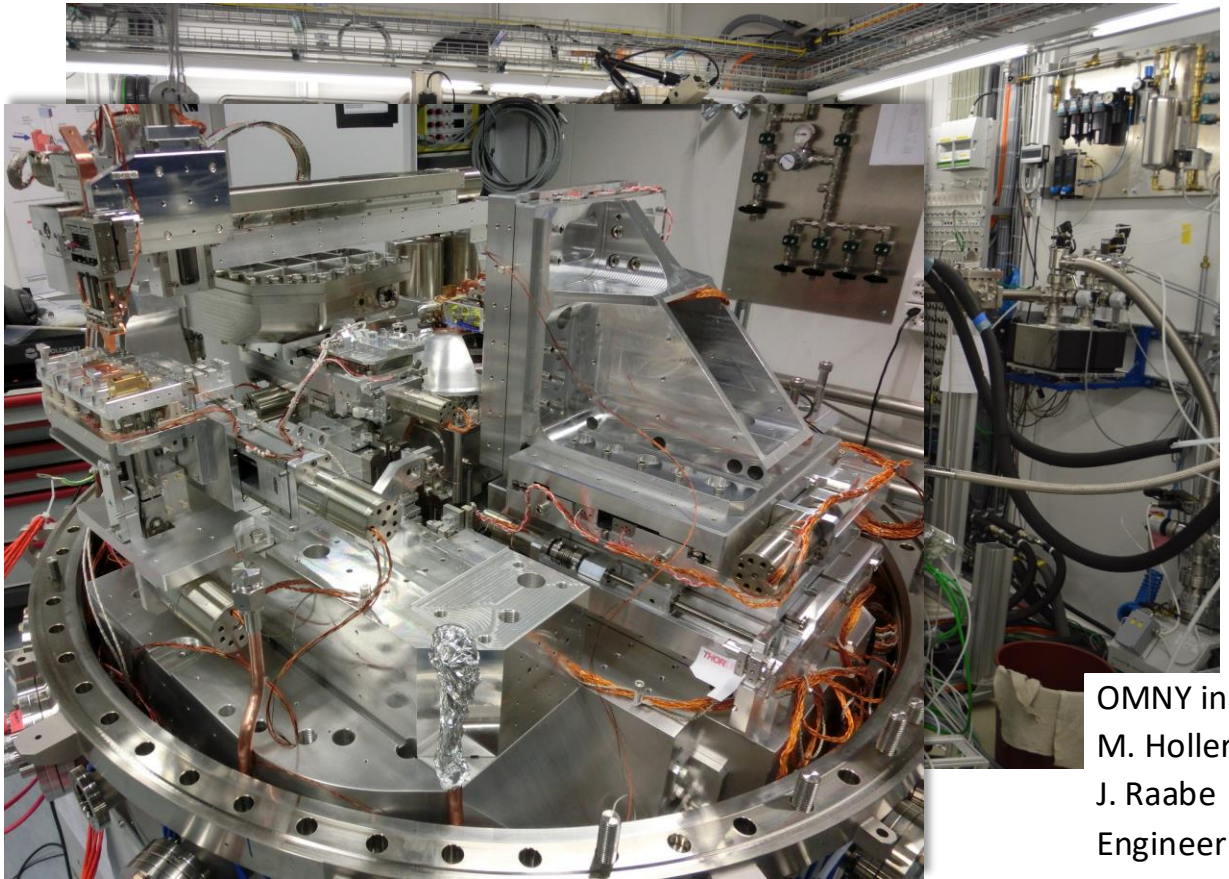

OMNY instrument SLS
M. Holler
J. Raabe
Engineer team at PSI

Ptychography at cryogenic temperature

Cyphochilus

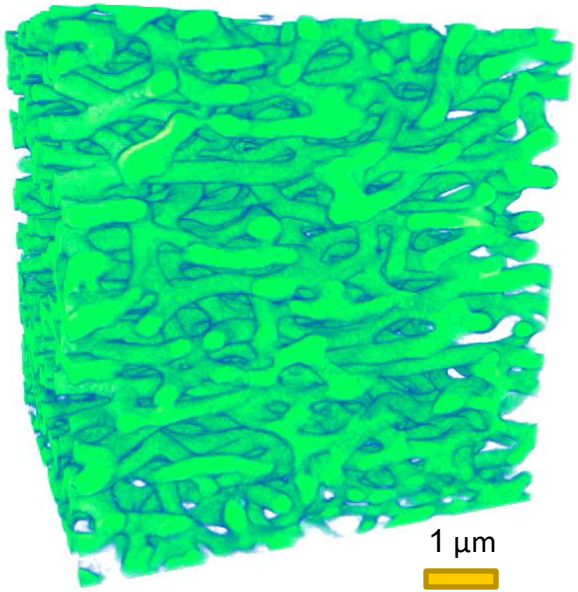

Radiation sensitive biological structure – Not measurable under non-cryogenic conditions.

Measured at 92K +/- 0.4 mK

Holler, M. *et al. Review of Scientific Instruments* **89**, 043706, (2018).

Bodo D. Wilts, *et al Advanced Materials*

Ptychography:
Quantitative mass density values

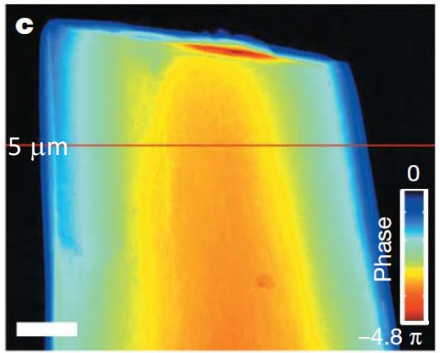

phase shift:

$$\phi(x,y) = -\frac{2\pi}{\lambda}\int \delta(\mathbf{r})dz$$

electron density: $n_e(\mathbf{r}) = \dfrac{2\pi\delta(\mathbf{r})}{\lambda^2 r_0}$

away from absorption edges!

mass density: $\rho = \dfrac{n_e A}{N_A Z}$

with A: molecular mass

Z: number of electrons in the molecule

Ptychography:
Quantitative mass density values

Demonstration of absolute density measurement

A. Diaz *et al.*, Phys. Rev. B **85** (2012) 020104(R)

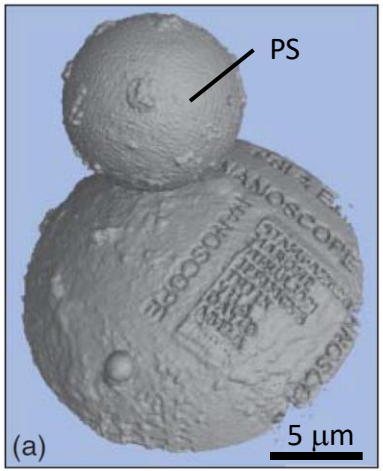

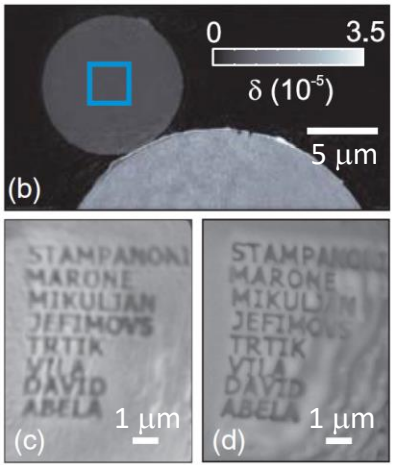

- Ptychographic tomography on test specimen
- Polystyrene sphere (PS) of 10 μm diameter with homogeneous density of **1.055 g/cm³**

- Measured density on PS based on gray values: **1.048 ± 0.008 g/cm³**
- (c) Spherical tomogram section
- (d) SEM image of the surface

Ptychography on hydrated cement paste

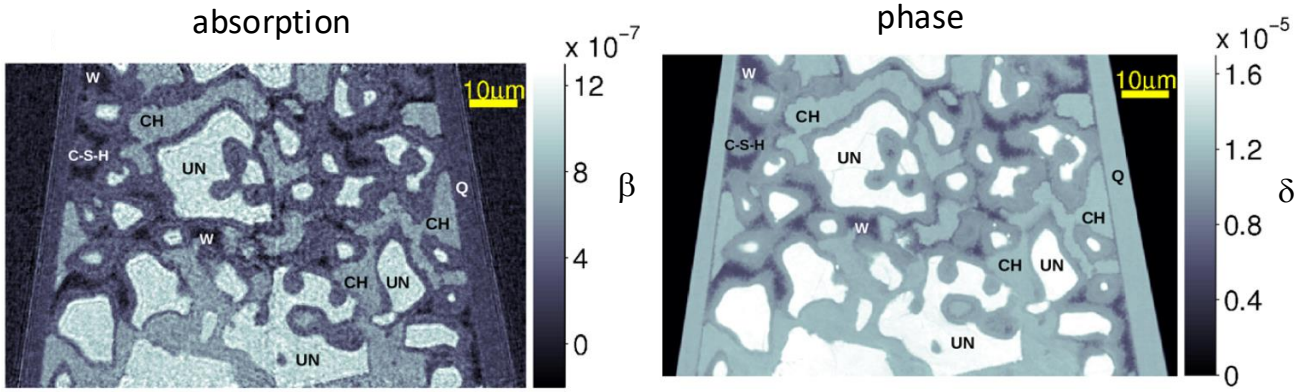

da Silva J, et al. *Langmuir* **31**, 3779 (2015).

Ptychography on hydrated cement – segmentation

bivariate histogram of absorption and phase information for segmentation

UN: unhydrated alite particles
W: porosity comprising mostly water
CH: calcium hydroxide
C-S-H: calcium silicate hydrates

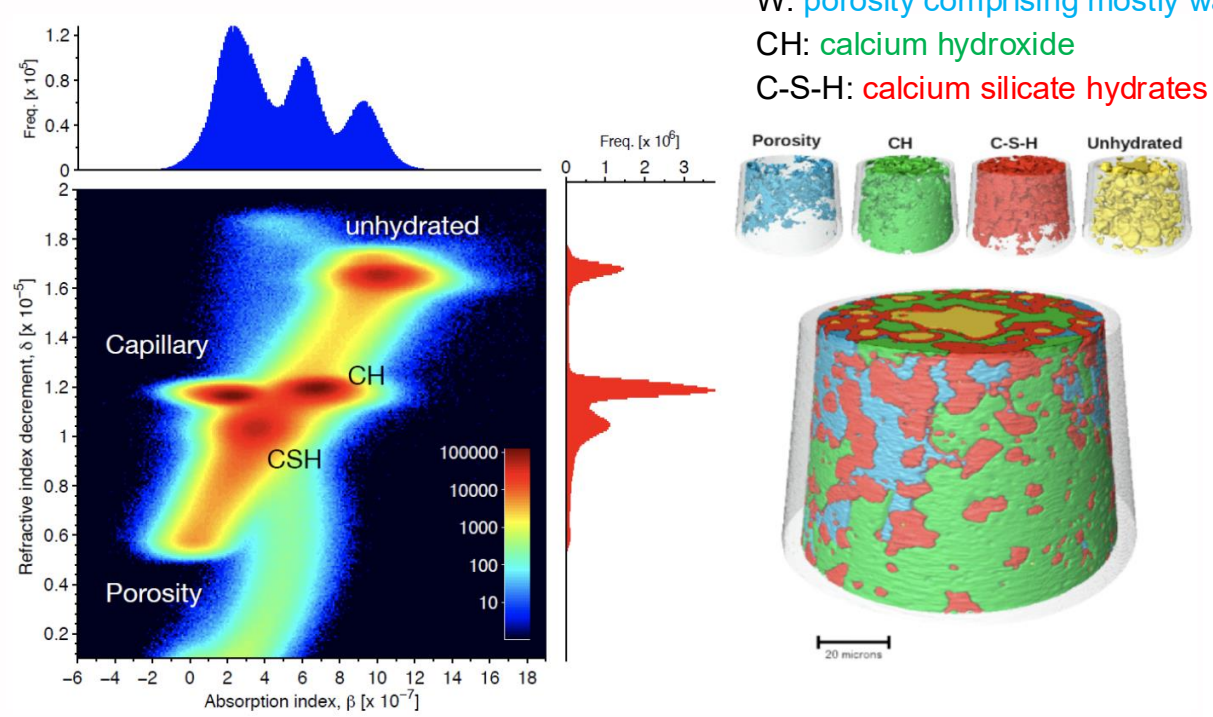

da Silva J, et al. *Langmuir* **31**, 3779 (2015).

Ptychography on hydrated cement – water content

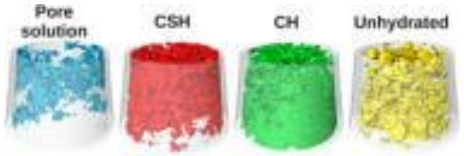

from quantitative mass density and stoichiometry,
the local water content could be determined

site-specific water content

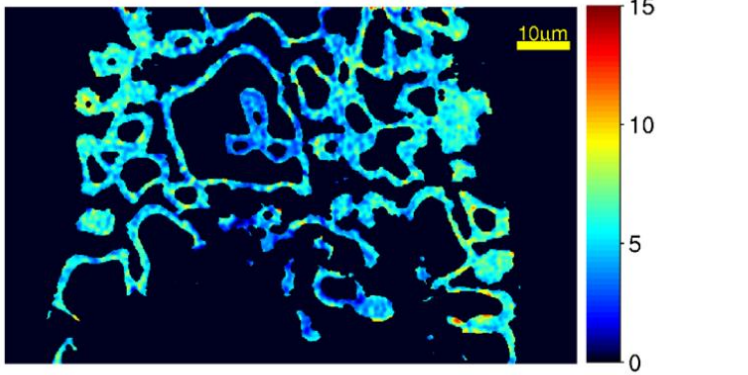

da Silva J, et al. *Langmuir* **31**, 3779 (2015).

Laboratory/Synchrotron µCT and Ptychography on cement

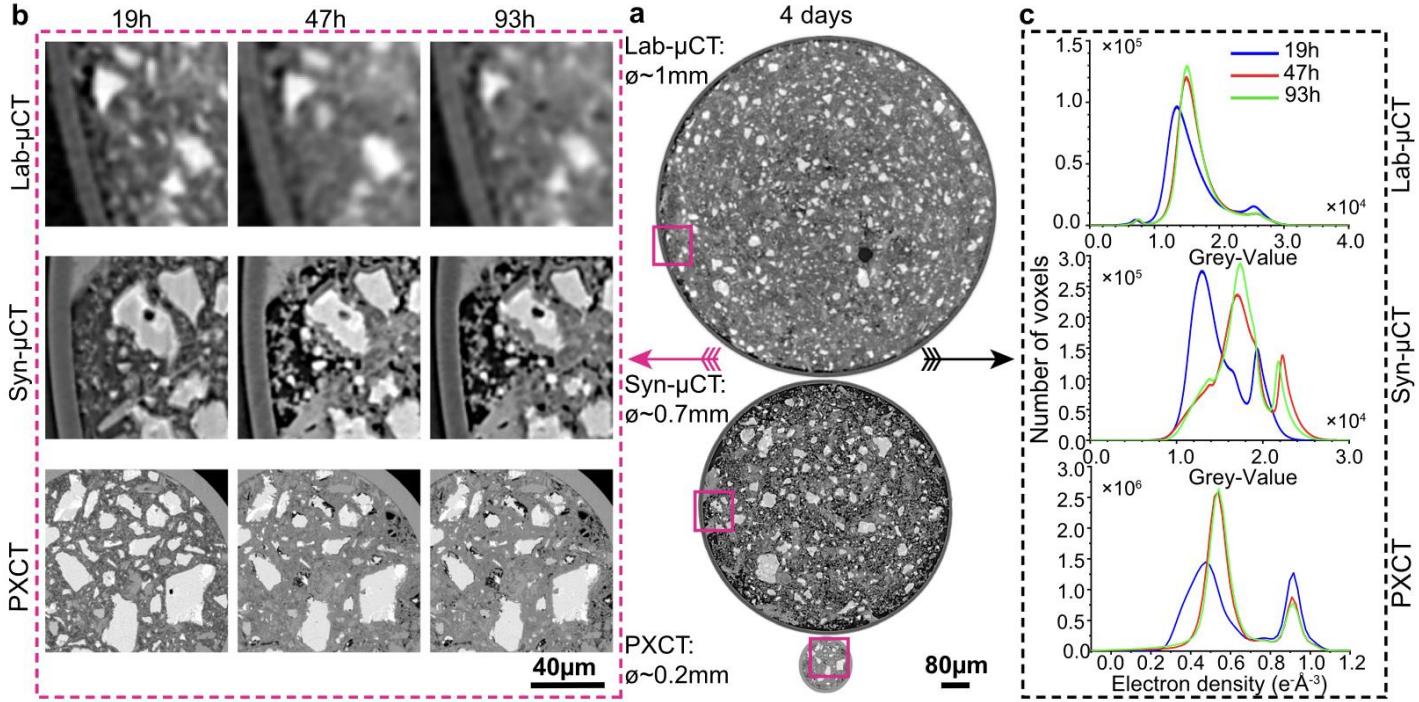

Shirani, S., et al. (2023). Nature communications https://doi.org/10.1038/s41467-023-38380-1

published May 8th 2023

Laboratory/Synchrotron µCT and Ptychography on cement

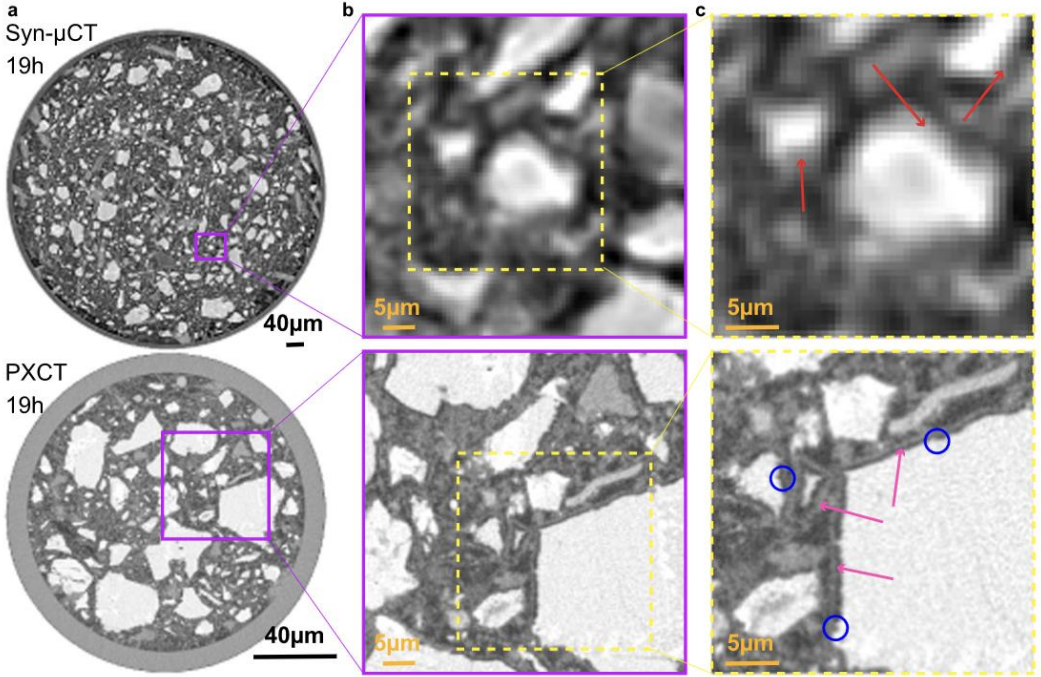

high resolution and contrast allows t resolve the C-S-H gel shells surrounding the alite particles (pink arrows) which is important to understand the mechanisms of cement hydration

Shirani, S., et al. (2023). Nature communications https://doi.org/10.1038/s41467-023-38380-1

published May 8th 2023

Ptychography on catalytic particles

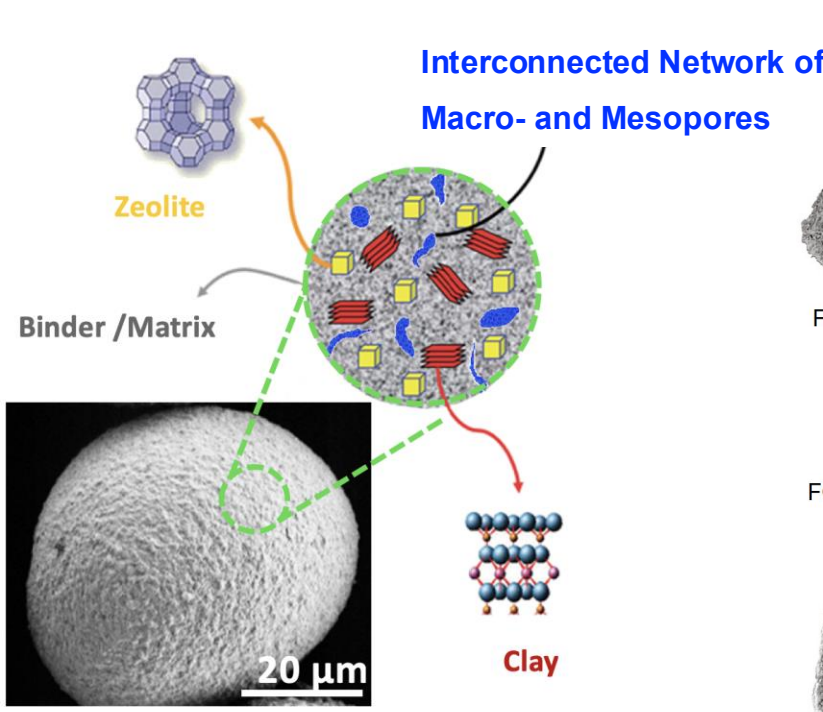

Adapted Figure- Perego and Millini *Chem. Soc. Rev.*, 2013, **42**

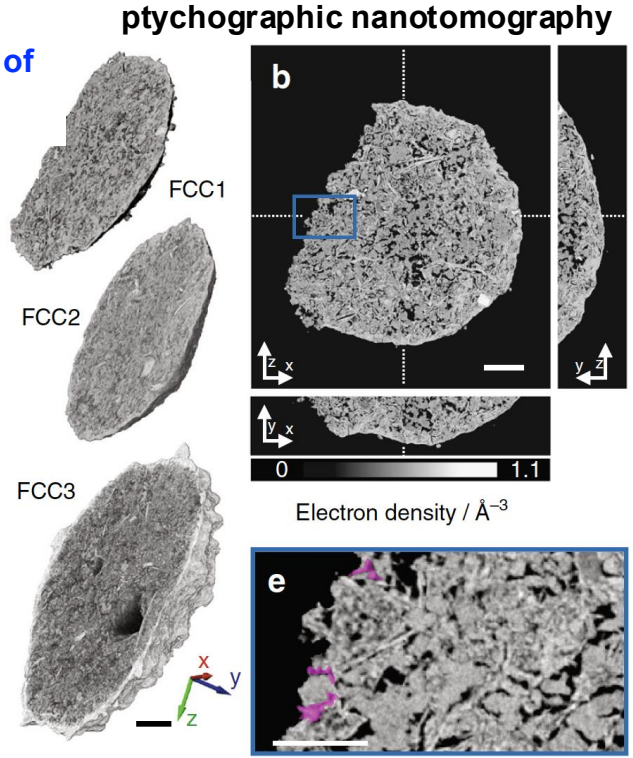

J. Ihli et al. *Nature Communication*, 2017, **8**, 809

Ptychography – resolution vs. pore size

Resolution by Fourier shell correlations 31 nm

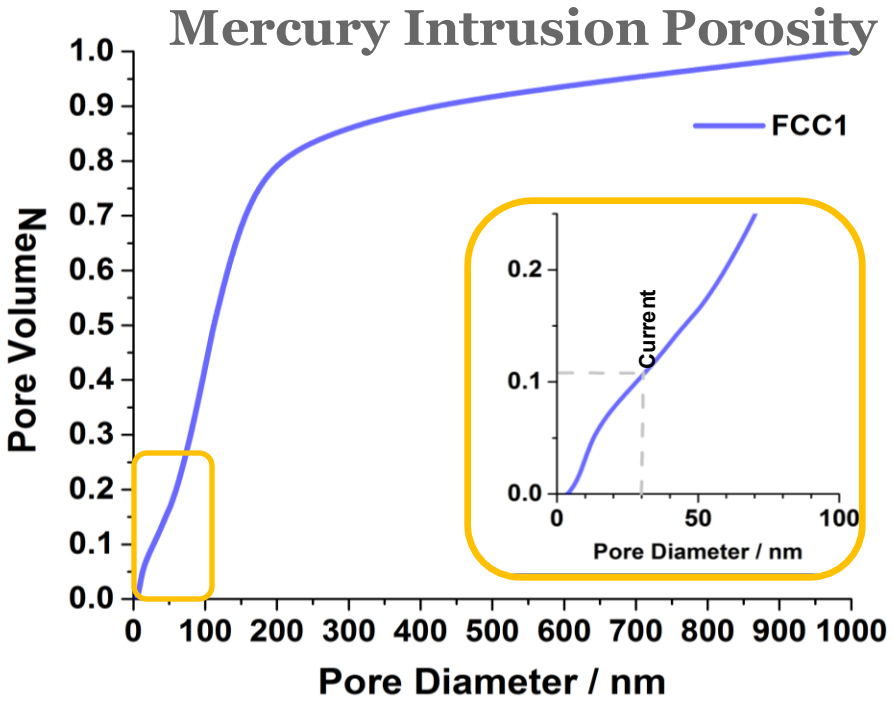

=> Tomograms probe a pessimistic **~90%** of the macro and mesopore volume.

J. Ihli et al. *Nature Communication*, 2017, **8**, 809

Ptychography on catalytic particle – component segmentation

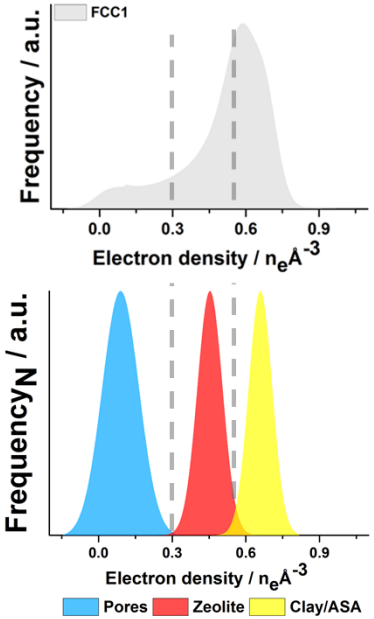

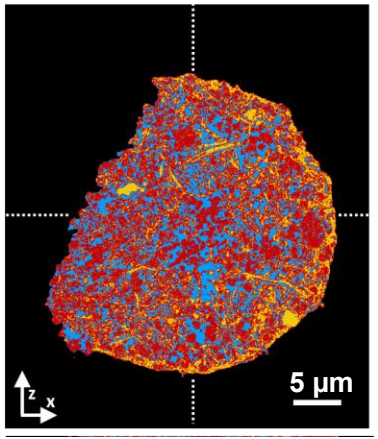

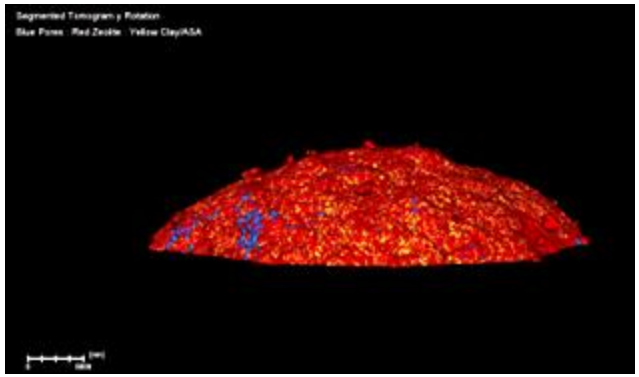

Pores (Grouping of Air and Hydrocarbons)

Clay/ASA (TiO_2, Clay and amorphous silica–alumina)

Zeolite

J. Ihli et al. *Nature Communication*, 2017, **8**, 809

Which particle is the most deactivated?

1 2 3

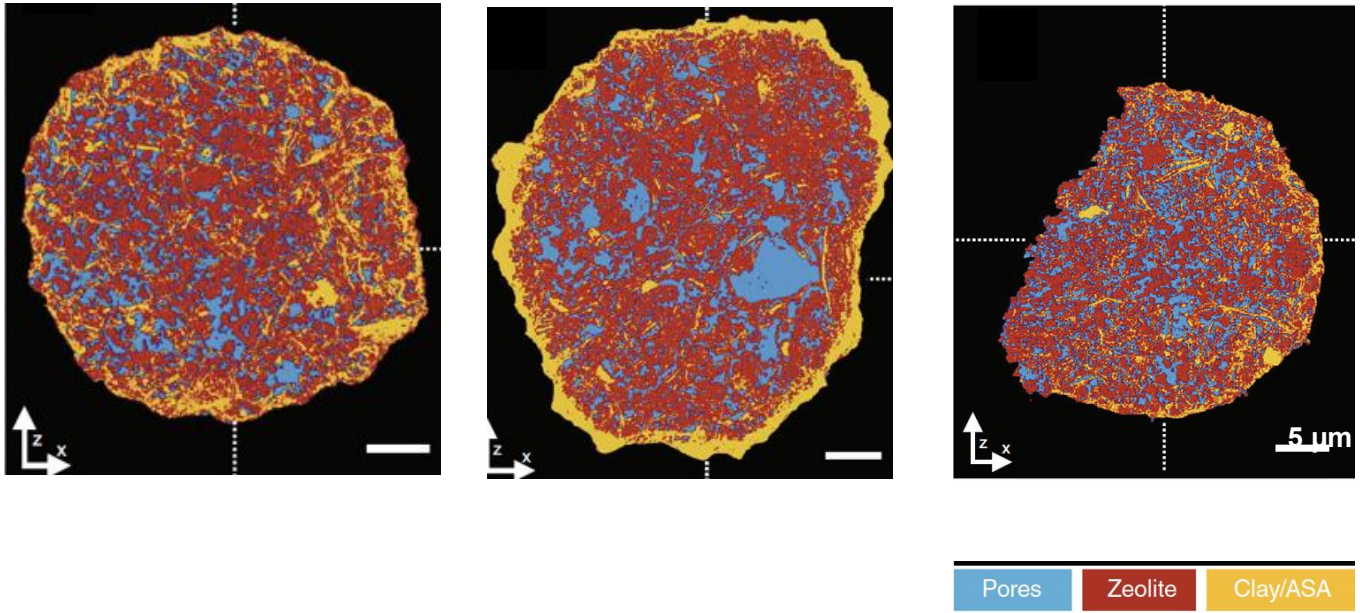

J. Ihli et al. *Nature Communication*, 2017, **8**, 809

Ptychography on catalytic particle – component segmentation

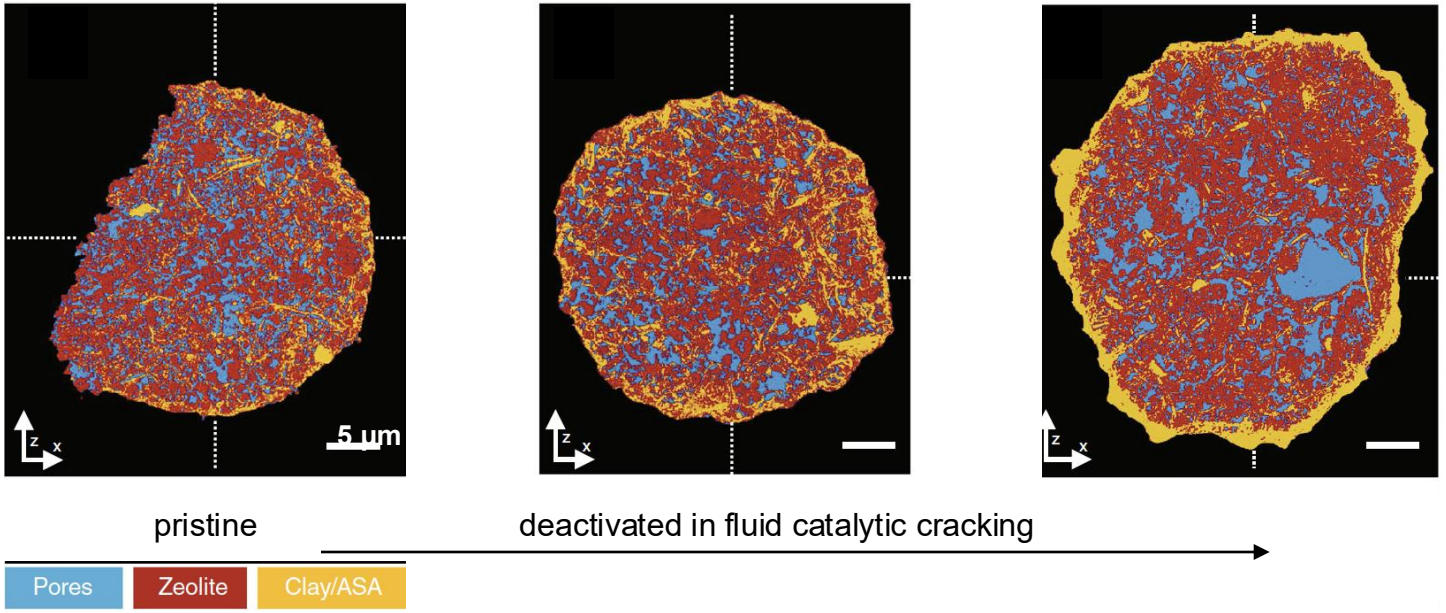

J. Ihli et al. *Nature Communication*, 2017, **8**, 809

Ptychography on catalytic particle – pore size analysis

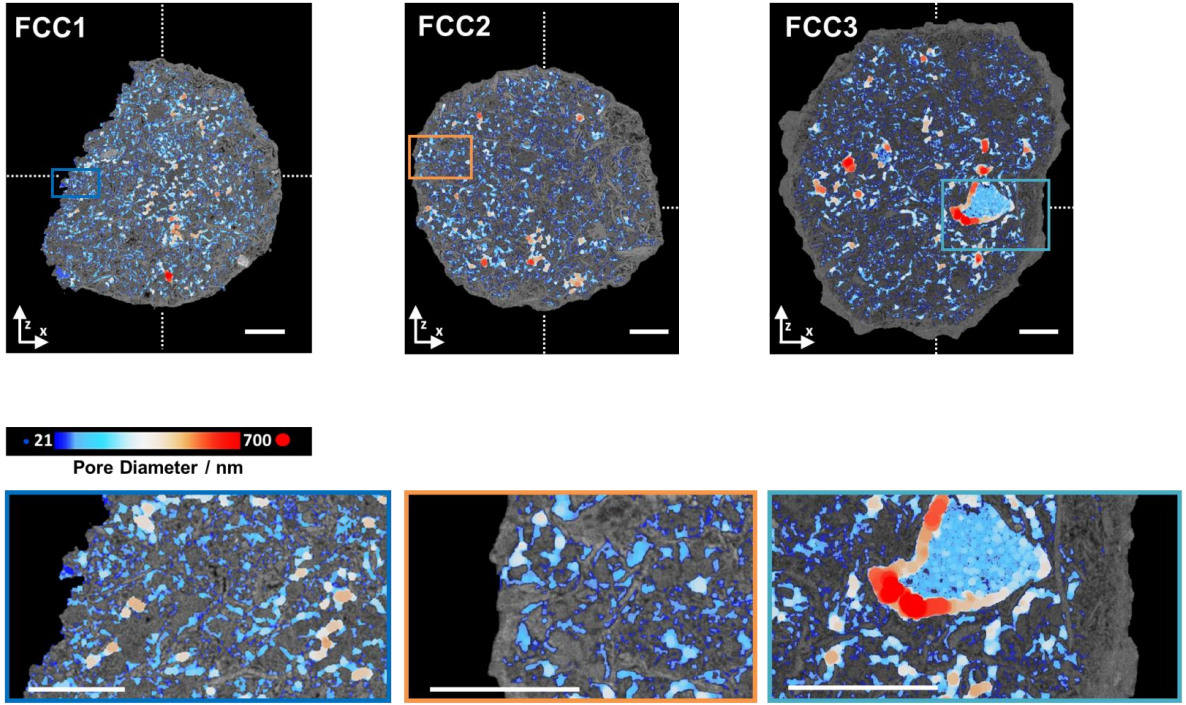

each porous region is fitted with maximal spheres filling this region best

J. Ihli et al. *Nature Communication*, 2017, **8**, 809

Ptychography on catalytic particle – pore size analysis and diffusion highways

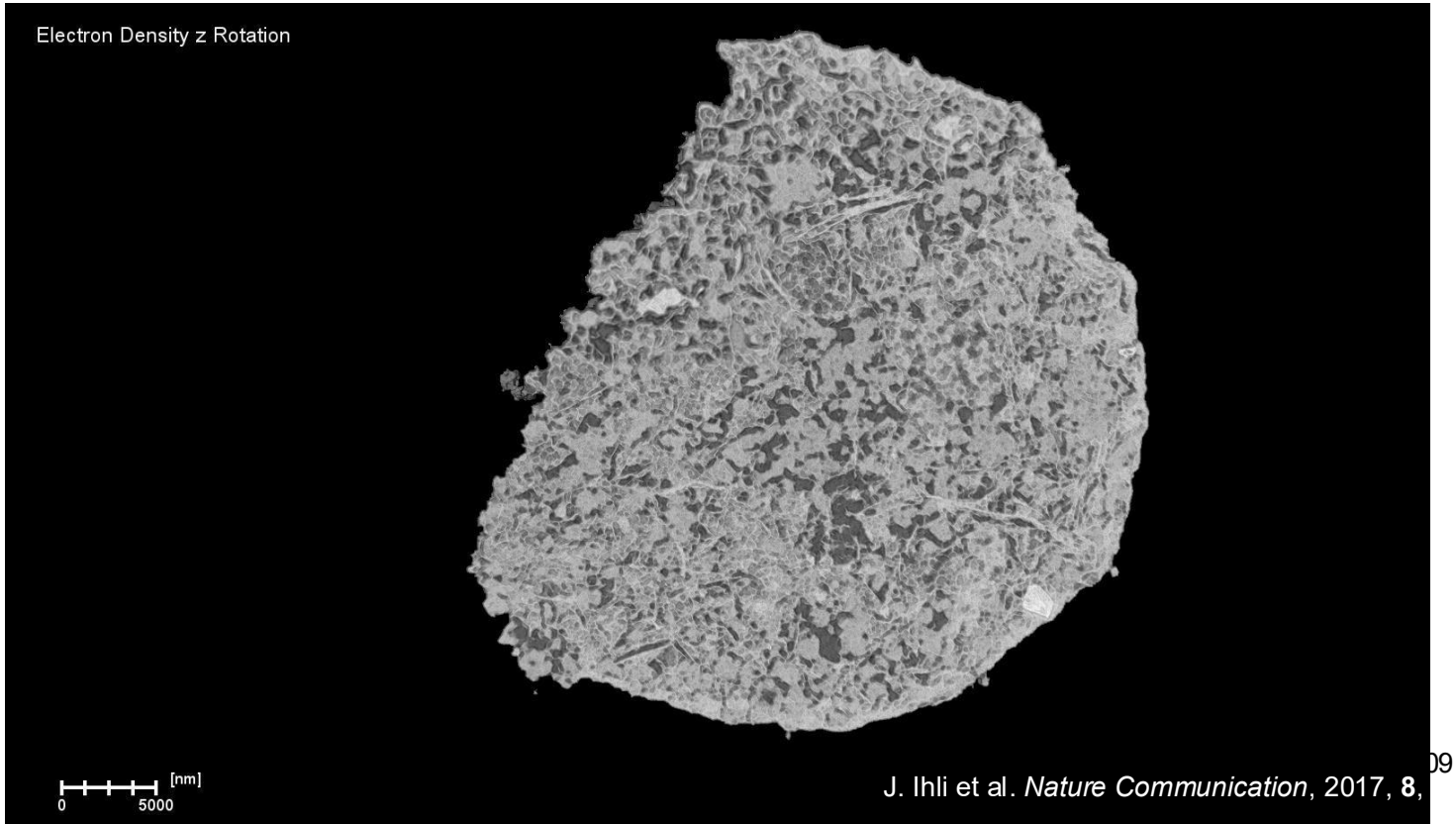

J. Ihli et al. *Nature Communication*, 2017, **8**, 09

XRD/XRF Tomography – on catalytic particle

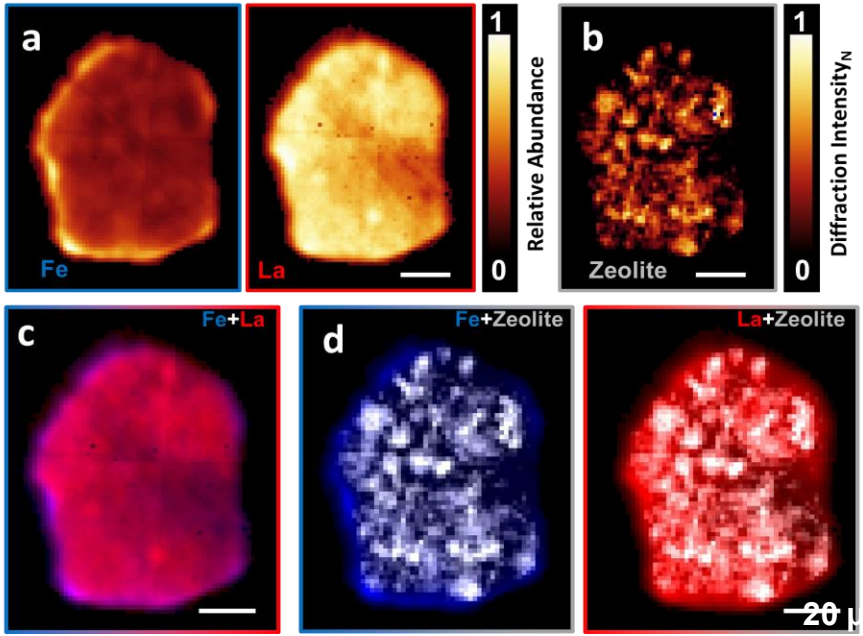

- Iron representative of amorphous silicia-aluminia shell
- Lanthanum representative of zeolites in pristine state (look into past)
- XRD current location of crystalline components

J. Ihli et al. *Nature Communication*, 2017, **8**, 809

Resonant Ptychographic Tomography

3D quantitative colocalization of chemical elements with physical features of functional matter with nanoscopic resolution.

Here colocalization of iron impurities within the primary components of a deactivated FCC catalyst. Spatial Resolution ~ 39 nm.

Acquired by means of a comparison of *on* and *off* resonance Fe-K edge ptychographic tomograms.

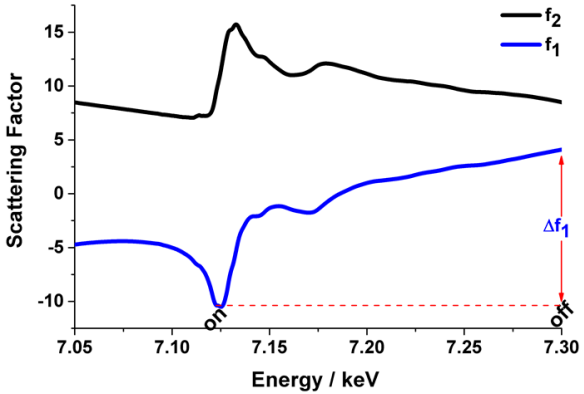

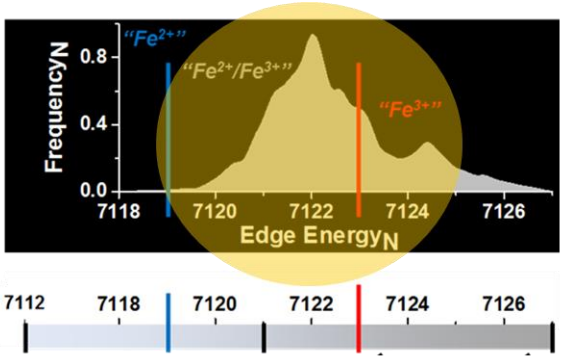

~ 95% of iron species in question posses a resonant energy of +- 2eV of the selected on-resonance energy !

Resonant Fe *K*-Edge Ptychographic Tomography

Deactivated Fluid Catalytic Cracking Catalyst (FCC3) measured electron density tomogram and iron distribution

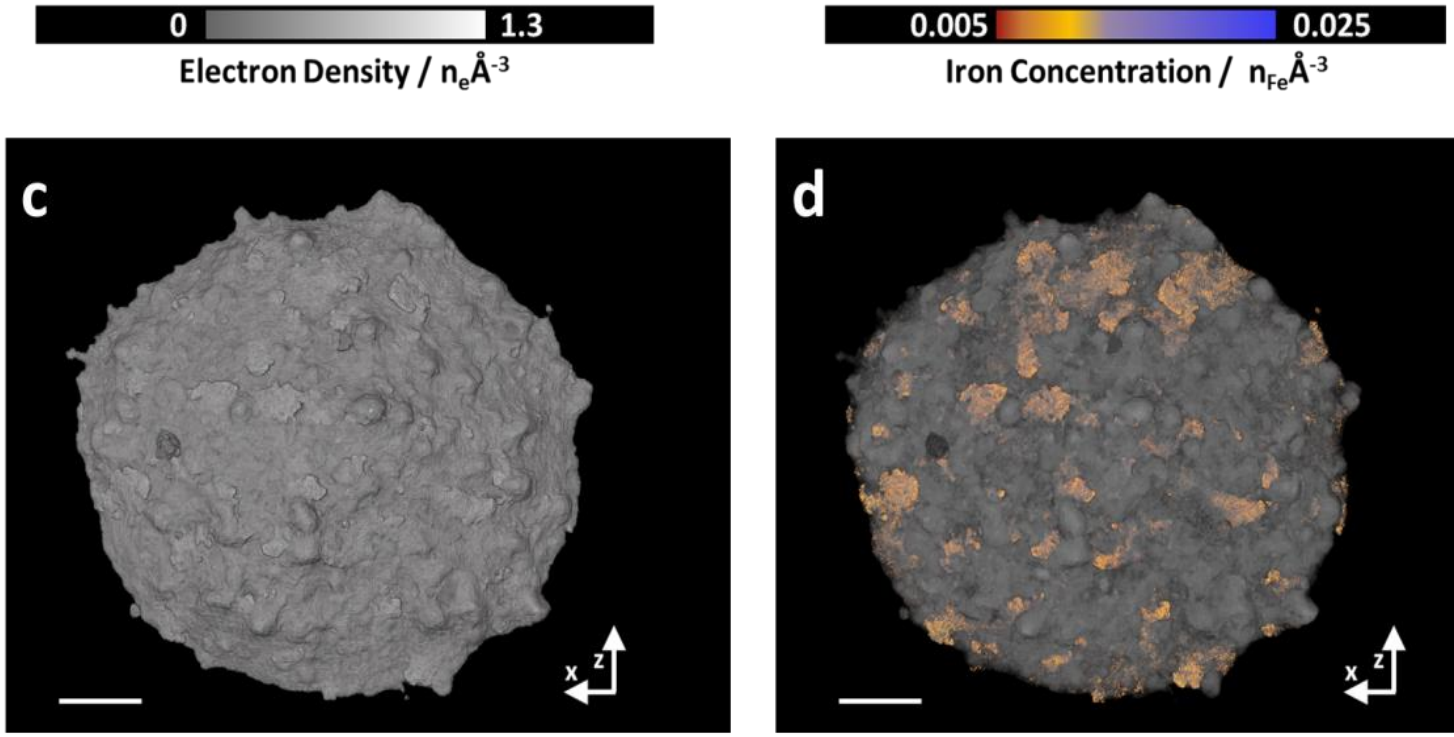

Resonant Fe *K*-Edge Ptychographic Tomography

Deactivated Fluid Catalytic Cracking Catalyst (FCC3) measured electron density tomogram and iron distribution

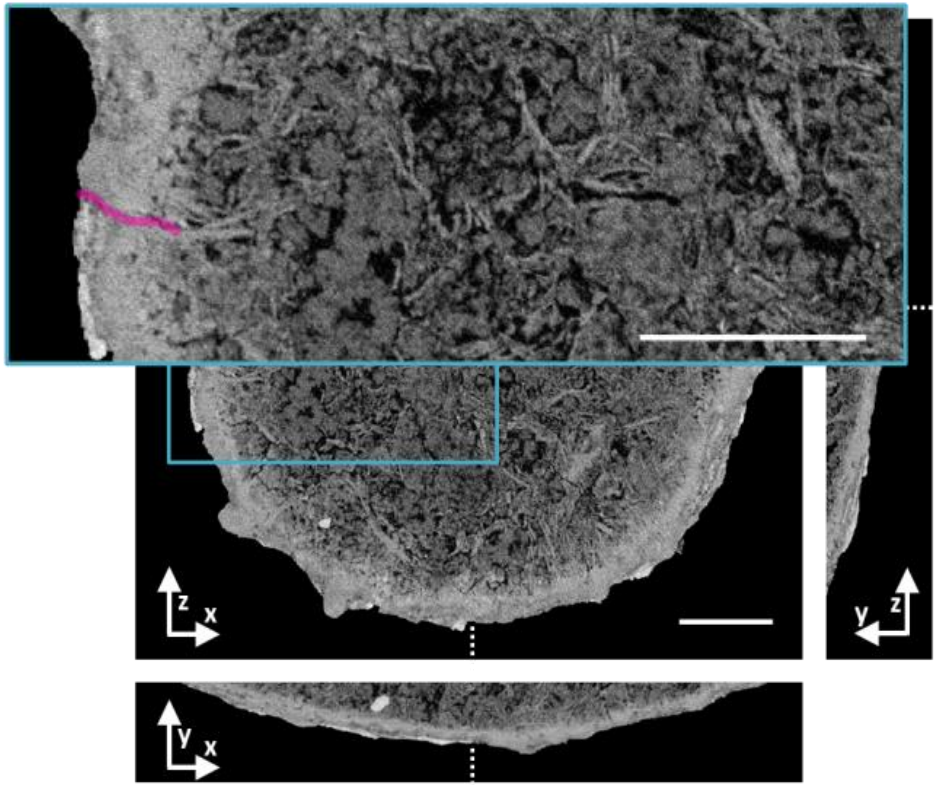

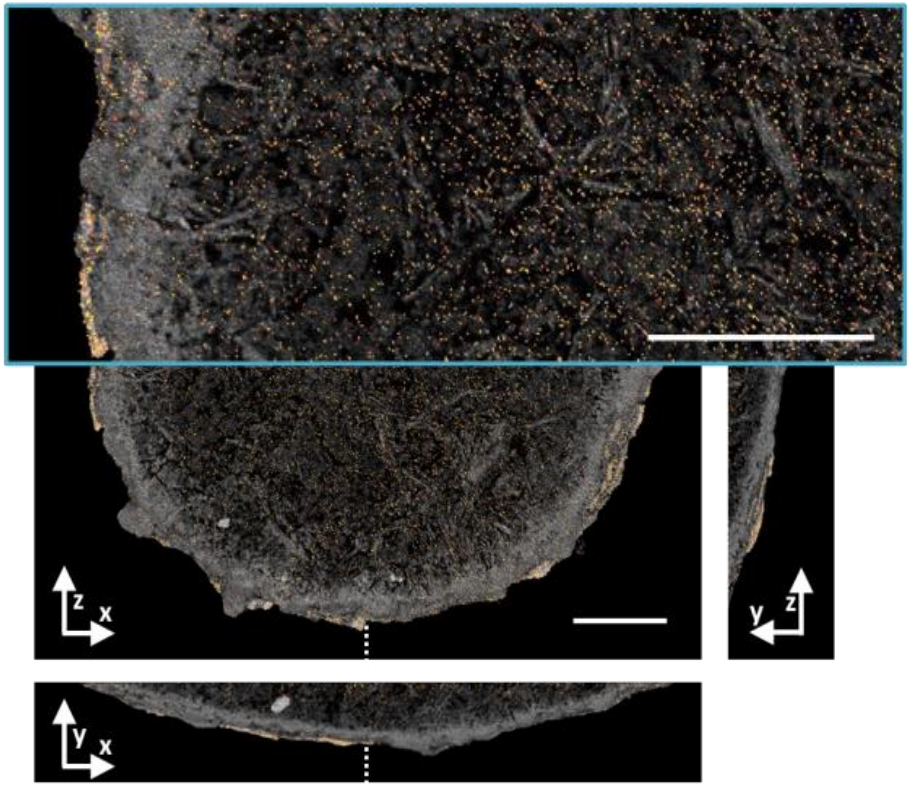

Combining Ptychography with XANES

Example spectra across vanadium K-edge

Chemical information

(ii) Vanadium concentration

(iii) Oxidation state

(iv) Coordination geometry (local crystalline order)

Combine with ptychotomo to obtain

3D nanoscale maps of chemical composition.

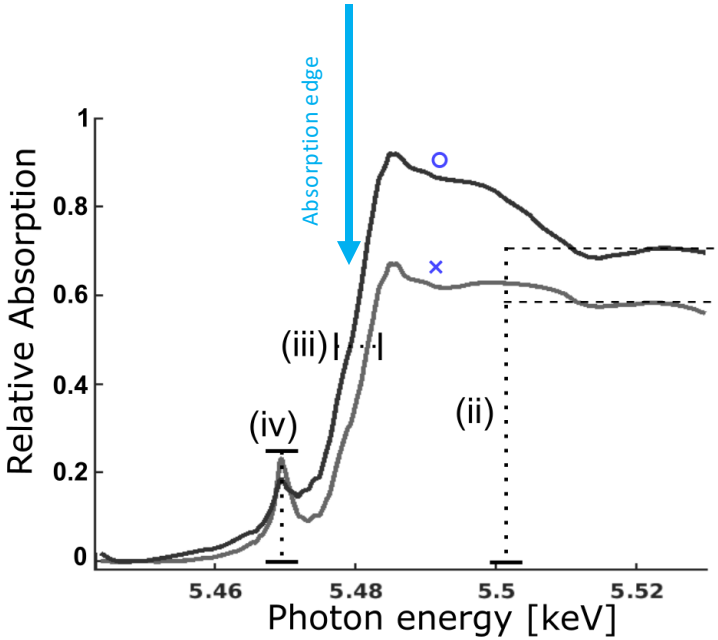

Sparse spectral ptychotomography on a VPO catalyst

Vanadium phosphorus oxides catalyst

Used in butane oxidation as prerequisite for household and industrial plastics (biodegradable)

10 micron diameter pillars

Chemical information, such as oxidation state can be obtained by measuring the X-ray transmission spectra

Combine with ptychotomo to obtain 3D nanoscale maps of chemical composition

Measuring one full tomogram per energy would be too slow

Gao *et al*, "Sparse ab initio x-ray transmission spectrotomography for nanoscopic compositional analysis of functional materials", Sci. Adv. **7**, eabf6971 (2021)

Sparse measurements

Number of projections needed in a tomography measurement is given by the *Crowther Criterion*:

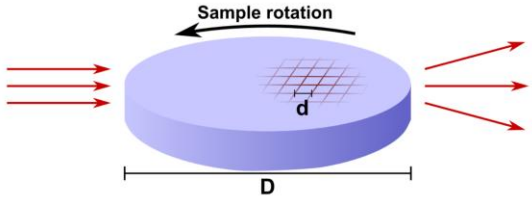

$$n_p = \frac{\pi D}{2d_{(half-period)}}$$

Conventional sampling of a full tomogram at each time frame / X-ray energy is too long, and not necessary

Information is sparse in multidimensional space

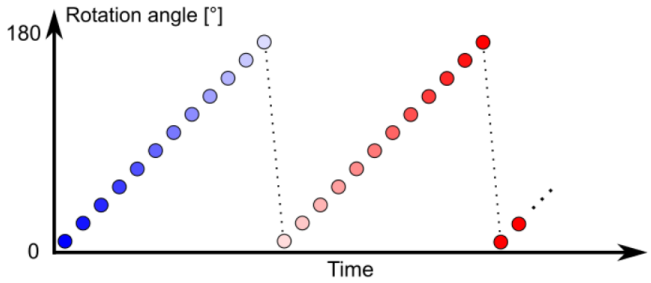

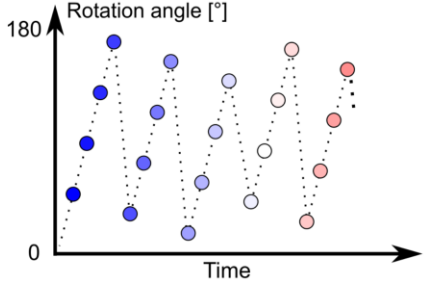

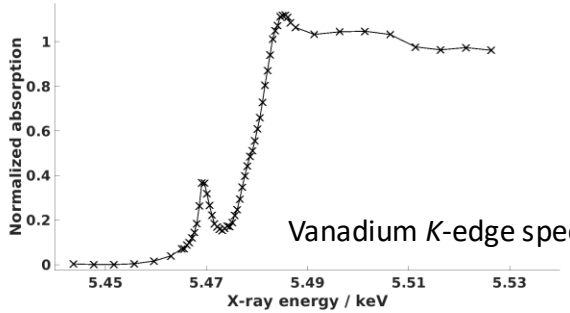

Vanadium *K*-edge spectrum

Gao *et al*, "Sparse ab initio x-ray transmission spectrotomography for nanoscopic compositional analysis of functional materials", Sci. Adv. **7**, eabf6971 (2021)

Sparse spectral ptychotomography on a VPO catalyst

Crucial to reconstruct hyperspectral volume <u>from all projections simultaneously</u>

- Measured at 60 energies between 5.443-5.465 keV, minimum step 0.5 eV
- Sparse angular sampling, **<u>11%</u>** of Crowther sampling criteria. About 1 day of measurement per sample.
- Leverage signal sparsity in the spectral dimension → Only a few spectral modes actually exist
- Novel iterative method for *<u>ab initio</u>* reconstruction. Combination of PCA and SART. Preserves resolution, quality and SNR

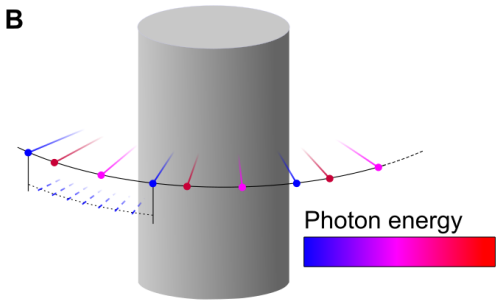

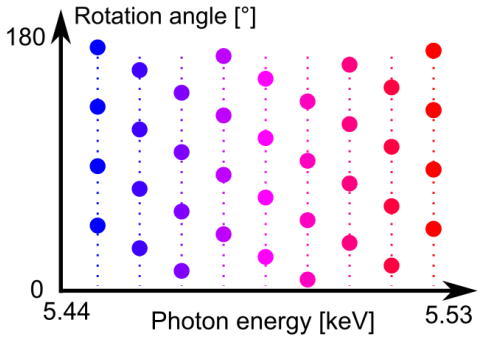

Gao *et al*, "Sparse ab initio x-ray transmission spectrotomography for nanoscopic compositional analysis of functional materials", Sci. Adv. **7**, eabf6971 (2021)

Sparse spectral ptychotomography on a VPO catalyst

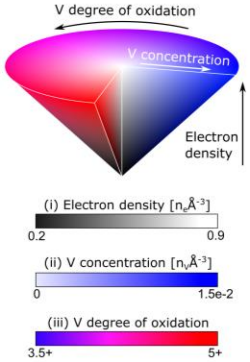

Pristine

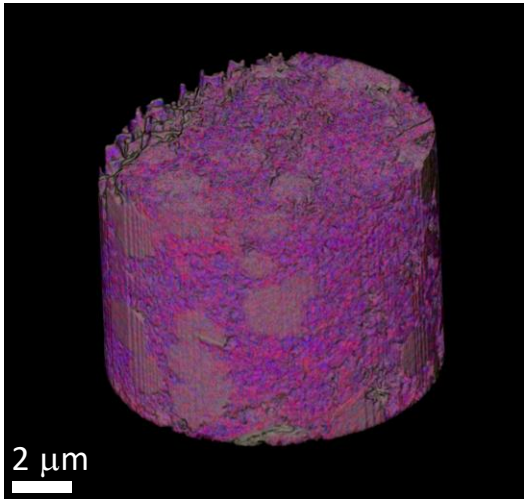

Used (4 years in industrial reactor)

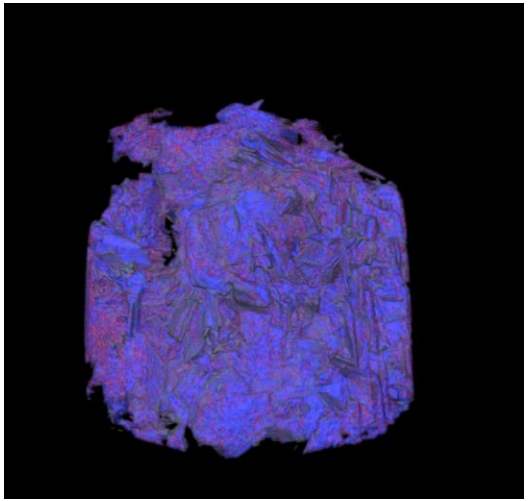

Hyperspectral tomogram resolution 26 nm

Gao *et al*, "Sparse ab initio x-ray transmission spectrotomography for nanoscopic compositional analysis of functional materials", Sci. Adv. **7**, eabf6971 (2021)

Sparse spectral ptychotomography on a VPO catalyst

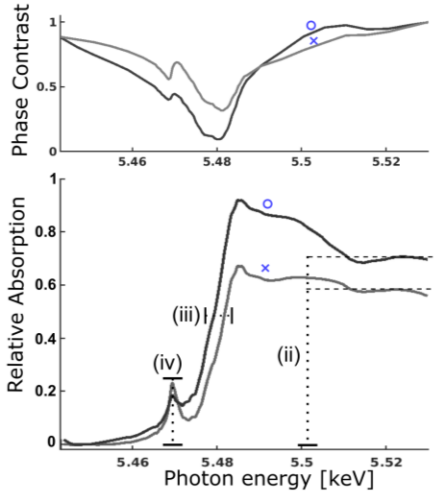

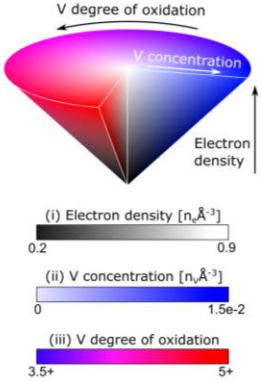

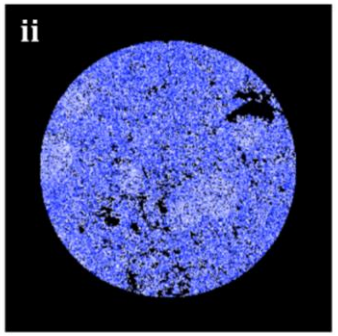

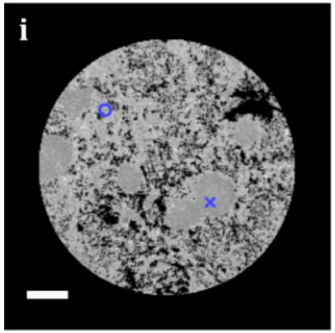

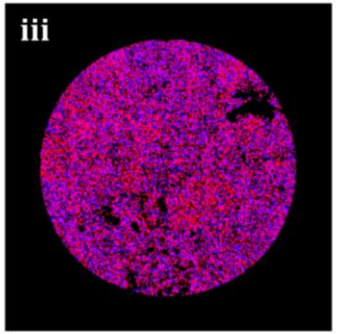

Gao *et al*, "Sparse ab initio x-ray transmission spectrotomography for nanoscopic compositional analysis of functional materials", Sci. Adv. **7**, eabf6971 (2021)

3D nanoscale maps of defects

Further analysis reveals **crystal structure defects** (vanadyl deficiencies) in the surface regions of the used catalyst sample. Thus far only theorized to exist as a possible active sites in the catalyzed reaction